NACA TN 4007

NATIONAL ADVISORY COMMITTEE FOR AERONAUTICS

TECHNICAL NOTE 4007

AN INVESTIGATION OF DISCHARGE AND THRUST CHARACTERISTICS OF FLAPPED OUTLETS FOR STREAM MACH NUMBERS FROM 0.40 TO 1.30

By Allen R. Vick

Langley Aeronautical Laboratory
Langley Field, Va.

NACA

Washington
July 1957

F

NATIONAL ADVISORY COMMITTEE FOR AERONAUTICS

TECHNICAL NOTE 4007

AN INVESTIGATION OF DISCHARGE AND THRUST CHARACTERISTICS OF FLAPPED OUTLETS FOR STREAM MACH NUMBERS FROM 0.40 TO 1.30

By Allen R. Vick

SUMMARY

The discharge and force characteristics of a group of flapped auxiliary air outlets, rectangular in cross section, have been investigated over a range of Mach numbers from 0.40 to 1.30. The results of this investigation are presented in a series of design charts. The ratio of outlet total pressure to stream total pressure required to attain a given discharge-flow ratio is shown to decrease markedly with increasing flap deflection and to vary strongly with the Mach number of the external stream. As the flap hinge point moved rearward, discharge-flow ratios were found to increase; flaps of aspect ratio 1 produced better discharge characteristics than those of aspect ratio 2. The force characteristics of these flapped outlets show that at a zero discharge rate the flaps of aspect ratio 2 have much lower drag than those of aspect ratio 1. The flaps of high aspect ratio have shorter chords with less of the flap exposed to the high-velocity air outside the boundary layer. At low discharge-flow ratios the difference between the measured thrust at any discharge-flow ratio and the measured drag at zero flow is generally much greater than that calculated from the momentum of the discharge air. This difference is obviously a result of the favorable effect of the jet on the drag characteristics of the flaps.

INTRODUCTION

The auxiliary air-flow requirements of aircraft have increased substantially in the past few years, and as a result, designers are being confronted with an increasing number of outlets, vents, drains, and such openings for which they must know the discharge and force characteristics. Although inefficient design of an individual outlet discharging small amounts of air may not seriously impair the aircraft performance, the cumulative effect of many outlets discharging large volumes of air (approaching 10 percent of that required by the engine) might produce significant penalties. Other problems arise concerning the most efficient means of bypassing large quantities of air around the engine for

purposes of matching the requirements of the air flow of the engine with the flow entering the inlet. For this problem the discharge and force characteristics of outlets must also be known if the most efficient design is to be achieved.

Discharge characteristics of outlets flush with the tunnel wall have been presented in references 1 to 3 for Mach numbers up to 1.30. Some force data obtained at a maximum Mach number of 0.1 are contained in reference 4, but the use of these data is somewhat limited because of the low maximum Mach number. A limited amount of force data on flush outlets at speeds higher than 0.1 are available in reference 3. The present investigation was undertaken to determine experimentally the discharge and force characteristics of flapped air outlets up to and through the transonic speed range. These data are presented in a series of design charts showing the variations of discharge and force characteristics of flapped outlets as a function of flap angle. The variables investigated include flap angle, hinge location, and aspect ratio. Duct pressure variations as a function of flap angle and Mach number are also presented. All tests were conducted over a Mach number range from 0.4 to 1.30.

SYMBOLS

A	minimum outlet area, sq ft unless otherwise noted
A_F	flap aspect ratio (ratio of flap span to flap chord)
C_T	measured thrust coefficient, T/qA
ΔC_T	apparent thrust coefficient, $C_T - C_{T(w=0)}$
l	total length of outlet parallel to stream, in.
M	tunnel Mach number
$p_{t,e}$	outlet total pressure, lb/sq ft
$p_{t,\infty}$	free-stream total pressure, lb/sq ft
p	static pressure, lb/sq ft
q	stream dynamic pressure, $\rho V^2/2$, lb/sq ft
r	radius of curvature of outlet, in.
T	thrust, lb

u velocity within boundary layer, ft/sec

V stream velocity, ft/sec

w outlet-discharge mass-flow rate, slugs/sec

x distance downstream from front of outlet, in.

y distance perpendicular to surface, in.

ρ tunnel air density, slug/ft^3

δ boundary-layer thickness, in.

δ_f flap angle, deg

$\frac{w}{\rho VA}$ discharge-flow ratio,

$$\frac{\text{Outlet discharge flow}}{\text{Tunnel discharge flow through area equal to outlet area}}$$

C_p pressure coefficient,

$$\frac{\text{Duct static pressure - Free-stream static pressure}}{p_{t,\infty}}$$

δ^* boundary-layer-displacement thickness, $\int_0^\infty \left(1 - \frac{u}{V}\right)dy$

θ boundary-layer-momentum thickness, $\int_0^\infty \left(1 - \frac{u}{V}\right)\frac{u}{V}\,dy$

H boundary-layer-shape parameter, δ^*/θ

APPARATUS AND PROCEDURE

The transonic tunnel used in this investigation has a rectangular test section $4\frac{1}{2}$ inches high, $6\frac{1}{4}$ inches wide, and 17 inches long as is shown schematically in figure 1. The plenum chamber below the slotted bottom wall of the tunnel was connected to a vacuum pump, and the speed for Mach numbers above 0.95 was varied by adjustment of the rate of air removal from the chamber. The top wall was solid, with a rectangular shaped cutout in which the combination outlet and force dynamometer was mounted. All flaps, therefore, projected downward from the top wall of

the tunnel. The outlet air was supplied from upstream of the test section at a total pressure always less than the tunnel total pressure. A metering nozzle mounted in the supply pipe was used to determine the mass flow through the outlet.

The basic outlet configuration used in this investigation was the same for all tests, the individual flaps being attached as shown in figure 2. Both the upstream and downstream ends of the rectangular shaped outlet were curved and had a 2-inch radius tangent to the surface. The length l of the outlet was 1.865 inches, and the location of the hinge line x was the distance measured downstream from the front of the outlet. Other significant dimensions of the outlet are also given in figure 2. Thirteen different models were tested with flap angles varying from approximately 0° to 37°. Nine of the flaps tested were of aspect ratio 1 and four were of aspect ratio 2. Because the outlet and flap width were held constant at 1 inch, a change in aspect ratio was achieved by using flaps with shorter chords. For these tests the flap hinge position was changed three times and is expressed as the ratio of flap-hinge-point location (measured from the outlet front) to total outlet length x/l.

The outlet area A is defined as the minimum cross-sectional area between the downstream end of the flap and the outlet wall. Figure 3 shows the variation of outlet area with flap angle for the different flap aspect ratios and flap-hinge-line locations.

In these tests discharge and force data were recorded cohtinuously on automatic data plotters as a function of stream Mach number. All pressures required to obtain discharge and stream characteristics were connected to individual pressure cells and then transmitted electrically to continuously recording, null-balance, potentiometers. Pressure leads to the various pressure cells were kept short to minimize any time lag. The tunnel total pressure was measured at a point in the duct upstream of the test section, and the stream static pressure was measured at a point just upstream of the outlet. These two pressures together with the stream total temperature defined the stream conditions. The outlet discharge rate was obtained from pressures recorded from pipe taps in the outlet air-supply line upstream and downstream of the metering nozzle. (See fig. 1.) A pressure tap in the air-supply line just upstream of the outlet was used to obtain the outlet total pressure.

The force dynamometer was of the floating-body type previously described in reference 3. This balance, rectangular in shape, is shown schematically in figure 2. Basically, it consists of a floating body supported by two flat cantilever springs. All axial loads, either drag or thrust, are transmitted through the springs to unbonded strain-gage elements and from there to the continuously recording potentiometer. A small clearance gap surrounds the floating body. The larger air gap, as shown in detail A (fig. 2), was for the purpose of allowing any pressure

differential that might exist between the upstream and downstream end of the balance to equalize and thereby minimize the tare force. Two unbonded strain gages were used. The strain gages were balanced both mechanically and electrically to compensate for any temperature changes. The maximum movement of the floating body at full load was 0.0015 inch. A labyrinth seal separated the top of the floating body and the outlet air-supply line. This gap was kept as small as possible and was calibrated for leakage flow as a function of the pressure ratio in the outlet chamber. All data have been corrected for this slight leakage flow. The floating part of the balance was insulated from the tunnel, and a light was installed to warn of any contact between the balance and surrounding areas.

The methods used to obtain the data usually required a maximum of six separate tests for each model at values of discharge flow ranging from zero to a maximum. Before each test the valve in the outlet air-supply line was set for a given mass flow. The speed was increased slowly from a Mach number of zero, and data were recorded continuously with increasing speed, a time interval of 3 to 4 minutes being required to cover the entire Mach number range. After each test the speed was decreased to zero and the valve setting was changed to give a different outlet discharge-flow rate. Data recordings were always made with speed being increased in order to maintain a consistent method of testing. Check runs made with the speed being decreased showed only minor differences in results.

Since all outlets are either partly or completely submerged in the boundary layer at the tunnel wall, it is apparent that the conditions under which this investigation was conducted are of interest to the designer. The characteristics of the boundary layer measured at a point on the tunnel wall just upstream of the flaps are shown in figure 4 as a function of stream Mach number. Each of the boundary-layer parameters, δ, δ^*, θ, and H, decreases with increasing speed.

RESULTS AND DISCUSSION

The discharge and drag characteristics of the outlets at Mach numbers from 0.4 to 1.30 are presented in figure 5. In each part of figure 5 the discharge-flow rate is presented nondimensionally as the ratio of outlet discharge flow to the tunnel discharge flow through a stream tube having a cross-sectional area equal to that of the outlet. This outlet discharge-flow ratio is presented as a function of the ratio of outlet total pressure to stream total pressure $p_{t,e}/p_{t,\infty}$. The outlet drag (or thrust) is also presented in figure 5 in coefficient form as a function of the discharge-flow ratio $w/\rho VA$. Because the testing technique adopted for this investigation resulted in simultaneous variations

of stream Mach number, outlet-pressure ratio, and discharge-flow ratio, these curves were obtained from cross plots; accordingly, no data points appear in these figures.

For a flap angle of approximately 0°, comparisons show that the ratio of the outlet total pressure to the free-stream total pressure at zero flow $\left(\frac{w}{\rho VA} = 0\right)$ is very close to the ratio of free-stream static pressure to total pressure as obtained from compressible-flow tables at the desired Mach number (ref. 5). As the flap angle is increased, however, the outlet-pressure ratio decreases below the free-stream pressure ratio. A comparison of the slopes of the individual curves for a constant Mach number at different flap angles in figure 5 reveals that, below discharge-flow ratios of approximately 0.6, the rate of change of $w/\rho VA$ with $p_{t,e}/p_{t,\infty}$ for Mach numbers equal to or greater than 1.00 is essentially independent of flap angle. At Mach numbers less than 1.00 the rate of change is independent of flap angle below discharge-flow ratios of approximately 0.35. In these ranges the curves showing variations of $w/\rho VA$ with $p_{t,e}/p_{t,\infty}$ for each Mach number have approximately constant slopes. It seems probable that the discharge flow was primarily two-dimensional up to discharge-flow ratios of approximately 0.35 for Mach numbers less than 1.00 and 0.6 for Mach numbers equal to or greater than 1.00, but above these values a three-dimensional effect was introduced by air bleeding out on either side of the flaps, at $\delta_f > 0$, which thereby permitted a higher discharge-flow ratio at a constant outlet-pressure ratio. Since the outlet air was supplied at a pressure always equal to or less than the tunnel total pressure, the available pressure ratio can never exceed a value of unity. It should be noted that the discharge-flow ratio will increase with outlet-pressure ratio without limit since, even after choking, the mass of air being discharged continues to increase with outlet total pressure as a result of the increasing density.

The thrust coefficients shown in figure 5 for values of constant Mach number are based on the same minimum outlet area that was used in the mass-flow calculations. Negative values of the thrust coefficient indicate drag. With no air being discharged from the outlet ($w/\rho VA = 0$), the drag of the outlet varies with flap angle; that is, an increase in flap angle produces a corresponding increase in drag. As air is discharged, however, a thrust force corresponding to the axial component of the momentum of the air leaving the outlet is produced. At discharge-flow ratios where the curves for the measured thrust coefficient interfere with each other (fig. 5), the spread of the curves is represented by hatching rather than by individual lines. Above discharge-flow ratios of approximately 0.5 the effect of Mach number becomes greater, and for most flaps a systematic decrease in C_T with increasing Mach number is noted. A comparison of data of figure 5 at the higher flap angles shows a reduction in Mach

number effect at high discharge-flow ratios with an increase in the spread of C_T occurring at low discharge-flow ratios.

Design Charts

Flow characteristics.- Design charts from which the pressure ratio required to obtain a given discharge-flow ratio may be read as a function of flap angle are presented in figure 6. These data were obtained by cross-plotting the basic data shown in figure 5. Charts are presented for Mach numbers from 0.40 to 1.30, for flap aspect ratios of 1 and 2, and for three flap-hinge locations. The specific flap angles for which data are available are shown by short vertical bars along the abscissa at each Mach number. Dashed sections of the curves at values of constant $w/\rho VA$ represent extrapolation of the data.

For a flap with an aspect ratio of 1 and the hinge line in the forward location ($x/l = 0$), the pressure ratio required to obtain a given discharge-flow ratio (figs. 6(a) and 6(b)) decreases markedly with increasing flap deflection. This decrease becomes relatively small for flap angles above 25°, and higher flap deflections are therefore of little advantage except as a means of increasing outlet area. The decrease in outlet-pressure-ratio requirements with increasing flap angle is a result of decreasing pressure on the downstream side of the flap, which in turn produces a pumping effect on the discharged air. The lines for different mass-flow ratios are generally parallel; thus, the rate of change of pressure ratio with flap angle for many configurations does not depend to any great extent on the discharge-flow ratio. Since the outlet area required for a given discharge-flow rate is inversely proportional to $w/\rho VA$, an increase in the available discharge-flow ratio with increasing flap deflection $\left(p_{t,e}/p_{t,\infty} \text{ being constant}\right)$ reduces the outlet area required.

Comparisons of the results in figures 6(a) to 6(f) show that moving the hinge point rearward in general increases the value of $w/\rho VA$ at given values of the pressure ratio and flap angle. Since the static pressure immediately behind the flap is lower than the free-stream static pressure, it is apparent that the outlet static pressure must increase with distance downstream of the flap. Thus, moving the hinge line forward subjects a smaller percentage of the total outlet area to the lower static pressure behind the flap, whereby the pumping is decreased. Although the discharge-flow ratio does increase at a constant pressure ratio because of the rearward movement of the hinge line, the actual mass of discharged air decreases as a result of a corresponding decrease in outlet area. At high flow rates a significant decrease is noted in the flap angles required to attain a given discharge-flow ratio as the hinge line moves rearward.

Changes in flap aspect ratio were achieved by reducing the chord length of the flap. Comparisons of data for flaps of aspect ratio 1 (figs. 6(a) to 6(f)) with those for flaps of aspect ratio 2 (figs. 6(g) to 6(j)) show that flaps of aspect ratio 1 produce better discharge characteristics than those of aspect ratio 2, which require a higher pressure ratio to achieve a given $w/\rho VA$. Also, as $w/\rho VA$ and δ_f increase, the pressure ratio required for the higher aspect ratio becomes increasingly greater. These higher pressure requirements are a result of the reduced pumping of the shorter flaps of aspect ratio 2 which lie more completely within the boundary layer. Since the ratio of flap height to boundary-layer thickness varies with changing aspect ratio, the pressure-ratio requirements may depend more on the boundary-layer thickness than on aspect ratio. Movement of the flap-hinge location produced the same effects as were previously shown for the flaps of aspect ratio 1.

Duct pressures.- In many applications auxiliary air outlets are intended for intermittent operation, in which case the pressure in the duct exhausted by the outlet may be an important factor from consideration of the drag or of the structural characteristics. These duct pressures are shown in coefficient form, with C_p plotted against Mach number for several flap angles in figure 7 at aspect ratios of 1 and 2. Negative duct pressure coefficients indicate that the pressures in the ducts are below free-stream conditions. In general, the duct pressure decreases below the free-stream static pressure systematically with increasing speed up to a Mach number of approximately 1.03 and then gradually increases as the speed is increased further. Values are negative for all flap angles except for the flaps of aspect ratio 2 at a flap angle of 0°, where the duct pressure becomes slightly positive at the high and low Mach numbers. A comparison of curves for aspect-ratio effects shows that larger negative values may be obtained by using the flaps of aspect ratio 1. These results indicate that flapped outlets are much more effective as a means of reducing the pressure in a duct than conventional flush outlets. Duct pressures which are below the stream static pressure by values up to 50 percent of the stream dynamic pressure may therefore be obtained simply by increasing the flap angle. Changes in flap-hinge location at a constant flap angle produce negligible effects in the duct pressure coefficient.

Force characteristics at $w/\rho VA = 0$.- The design of flapped outlets requires not only a knowledge of the outlet discharge characteristics but also of the force characteristics. Since there are times when no air is being discharged from the outlet, the designer must know both the drag due to the flaps at zero discharge and the thrust or drag produced when air is being ejected into the stream. All flapped outlets for which discharge characteristics have been presented were mounted in a force dynamometer in order to determine the resultant forces in a streamwise direction over a range of discharge-flow ratios and stream Mach numbers. The results of these tests at zero discharge rate are shown in figure 8.

Since an outlet will normally produce a thrust force, these data are presented in the form of thrust coefficient; negative values of C_T indicate drag. Results are given as a function of flap angle for different hinge-point locations, flap aspect ratios, and Mach numbers.

The curves of flap angle plotted against drag show a systematic increase in drag with increasing flap angle. A marked increase in the slope of curves of C_T plotted against δ_f (fig. 8) is noted at flap angles on the order of 5° to 7° for flaps of aspect ratio 1. At flap angles less than 5° to 7° the flaps are completely immersed in the boundary layer, and the drag variation is small. Once the angle becomes large enough for the flap to extend beyond the boundary layer, the slopes of the curves increase abruptly and approach constant values for flap angles greater than 15°.

As the hinge point of the flap is moved rearward (x/l increased), the drag coefficient increases considerably; the drag force, however, is unchanged. The changes in drag coefficient are due to a decrease in the cross-sectional area of the outlet which accompanies a rearward movement of the hinge line. The outlet area rather than the flap projected area has been used in nondimensionalizing the drag measurements in order to maintain consistency with the presentation of the discharge characteristics. The outlet cross-sectional areas which are shown in figure 3 as a function of flap angle facilitate conversions of C_T to other functions of flap area.

Outlets with flaps of aspect ratio 2 have much lower drag than those with flaps of aspect ratio 1, particularly at high flap angles where the drag produced is approximately 1/3 of that produced with the flaps of aspect ratio 1. In all instances, as the aspect ratio is changed, there is a corresponding change in outlet area; however, the flap projected area is much smaller in proportion than the change in outlet area. Perhaps the most important factor in this decrease in drag with increasing aspect ratio is the fact that a much larger percentage of the flap area is immersed in the boundary layer. As previously stated, a change in aspect ratio was made by varying the flap chord and keeping the width constant.

Force characteristics at $w/\rho VA > 0$.- The resultant force in a streamwise direction for various flapped outlets at different rates of discharge are presented in figure 9. The measured thrust coefficients vary greatly with the flap angle, hinge-line location, and aspect ratio. With low discharge-flow ratios the measured force was positive only at relatively low flap angles; as the discharge-flow ratio increases there is a corresponding increase in C_T and also in the minimum flap angle at which thrust rather than drag is obtained. In the range of these tests a thrust was measured regardless of flap angle at discharge-flow ratios of the order of 0.4 to 0.5 or greater. Increases in the negative

slopes of the curves of C_T against δ_f occur in the low Mach number range as the discharge-flow ratio increases; however, the slopes at low values of δ_f change to positive slopes at a Mach number of 1.30. In general, Mach number effects are very small at low values of discharge-flow ratio, the smallest thrust being produced at $M = 1.00$. At high discharge-flow ratios and flap angles up to approximately 15° there is a general decrease in C_T with increasing speed.

The decrease in the measured thrust coefficient produced by moving the flap hinge point rearward is primarily a result of decreasing cross-sectional area. Hinge-point location x/l has almost no effect on C_T for flap angles of 0°, but as the flap angle increases the effects become significant. Low-speed data by Rogallo (ref. 4) also showed a decrease in C_T as the hinge point was moved to the rear.

Effects of aspect ratio on the measured thrust coefficient of flapped outlets, for constant discharge-flow ratios, are also shown in figure 9. At constant deflection angles, flaps of aspect ratio 2 give appreciably higher values of C_T than flaps of aspect ratio 1 for angles in excess of 10°. This difference is partly a result of the lower drag coefficient of flaps of aspect ratio 2 at zero discharge; however, previous comparisons of the discharge characteristics at a constant total-pressure ratio have shown in figure 6 that larger flap angles are required for flaps of aspect ratio 2 to attain a given discharge-flow ratio. This requirement of higher flap angles reduces the apparent advantage of the flaps of higher aspect ratio. Since the area required remains constant, for a given discharge-flow ratio, a direct comparison of C_T determines which aspect ratio is most effective. It thus becomes possible, under certain conditions, to obtain a higher thrust with the flaps of aspect ratio 1. The set of conditions selected by the designer therefore determines which flap is superior from a consideration of thrust.

Comparison of Experimental With Calculated Thrust

Shown in figure 10 are curves of the apparent thrust coefficient as a function of discharge-flow ratio. The apparent thrust coefficient ΔC_T is defined as the difference between the measured thrust coefficient at any discharge-flow ratio and the thrust coefficient at zero flow. Maximum ΔC_T for any given discharge-flow ratio occurs at low flap angles for subsonic Mach numbers, a gradual decrease in ΔC_T occurring as δ_f is increased. These trends reverse at Mach numbers of 1.00 and 1.30 because there is an increase in maximum values of ΔC_T with increasing flap angle. Flap angle had the smallest effect at a Mach number of 1.00. At low discharge-flow ratios the rate of change of ΔC_T with δ_f is small, regardless of Mach number; however, as $w/\rho VA$ increases there is a continuous increase in slope, particularly in the low-speed range.

Also shown in figure 10 are theoretical curves of ΔC_T plotted against $w/\rho VA$ for each Mach number. The equation for the calculated thrust coefficient defined in terms of the momentum of the discharged air is given in reference 3. For discharge-flow ratios up to approximately 0.55 the experimental values of ΔC_T at all Mach numbers or flap angles are greater than the calculation predicts. At low flap angles and subsonic Mach numbers, the experimental ΔC_T is as much as 100 percent higher than the calculated thrust. This difference obviously occurs as a result of a decrease in the drag of the flaps, which is caused by a favorable effect of the jet of discharging air on the pressure on the downstream side of the flaps. This effect was also observed in reference 4.

CONCLUSIONS

From this investigation of the discharge and force characteristics of flapped outlets it is concluded that:

1. The pressure ratio required to attain a given discharge-flow ratio decreases markedly with increasing flap deflection.

2. Discharge-flow ratios increase as the flap hinge point moves rearward at a constant pressure ratio and flap angle.

3. Flaps of aspect ratio 1 produce better discharge characteristics than flaps of aspect ratio 2 as a result of the fact that a flap of higher aspect ratio has a shorter chord and less of the flap is exposed to the high velocity regions of flow.

4. Reducing the flap chord by one-half, thereby doubling the aspect ratio and reducing the flap projection above the wall boundary layer, reduces the drag at a zero discharge-flow ratio. Flaps of aspect ratio 2 generally yield a higher measured thrust coefficient over the entire mass-flow range; however, it is possible under certain conditions to obtain a higher thrust with flaps of aspect ratio 1.

5. The apparent thrust produced by the discharged air from flapped outlets is generally greater than that calculated from the momentum of the discharged air.

6. Duct pressures which are below the stream static pressure by as much as 50 percent of the free-stream dynamic pressure may be obtained with the flaps of low aspect ratio at high flap angles.

Langley Aeronautical Laboratory,
National Advisory Committee for Aeronautics,
Langley Field, Va., April 1, 1957.

REFERENCES

1. Nelson, William J., and Dewey, Paul E.: A Transonic Investigation of the Aerodynamic Characteristics of Plate- and Bell-Type Outlets for Auxiliary Air. NACA RM L52H20, 1952.

2. Dewey, Paul E.: A Preliminary Investigation of Aerodynamic Characteristics of Small Inclined Air Outlets at Transonic Mach Numbers. NACA TN 3442, 1955. (Supersedes NACA RM L53C10.)

3. Dewey, Paul E., and Vick, Allen R.: An Investigation of the Discharge and Drag Characteristics of Auxiliary-Air Outlets Discharging Into a Transonic Stream. NACA TN 3466, 1955.

4. Rogallo, F. M.: Internal-Flow Systems for Aircraft. NACA Rep. 713, 1941.

5. Ames Research Staff: Equations, Tables, and Charts for Compressible Flow. NACA Rep. 1135, 1953. (Supersedes NACA TN 1428.)

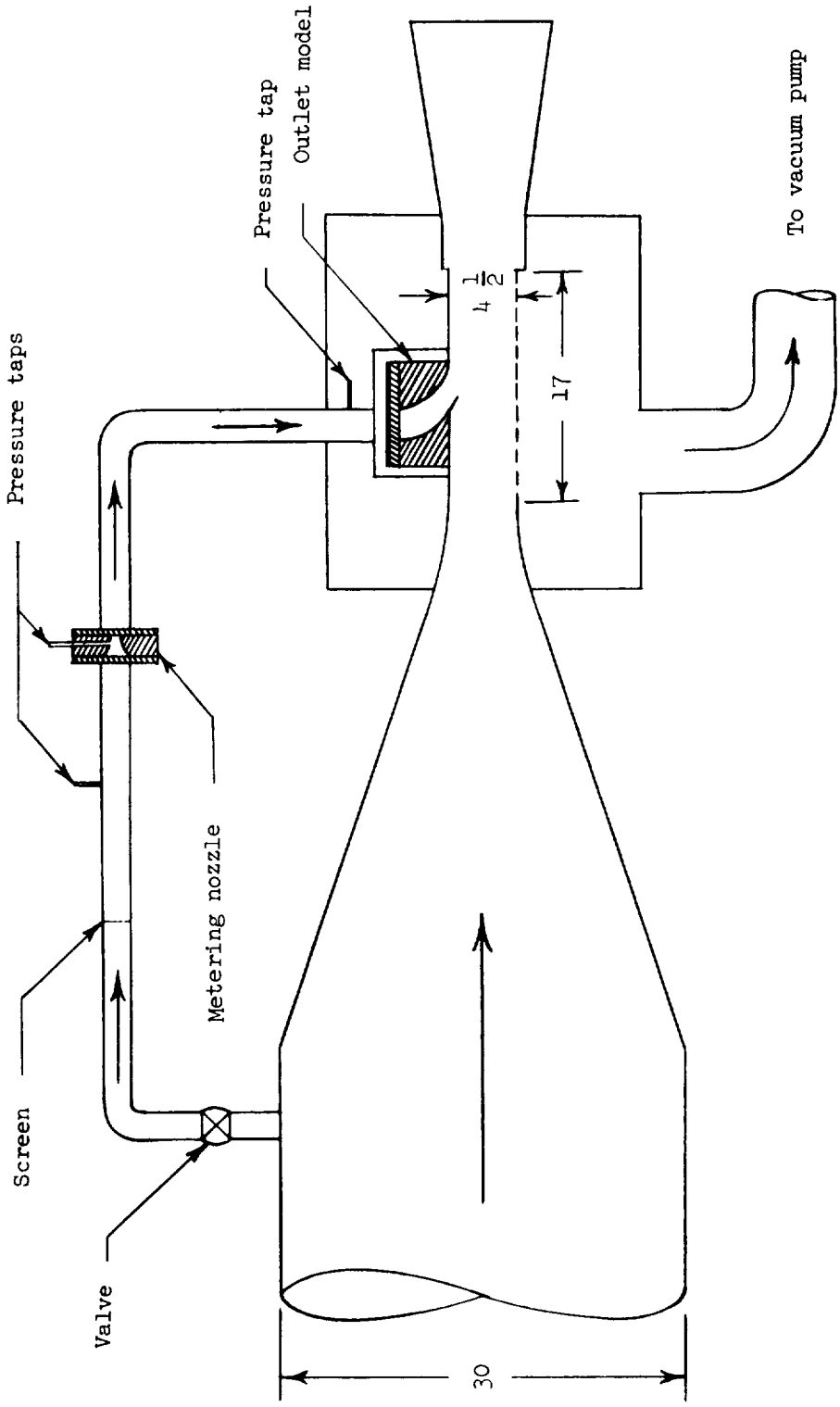

Figure 1.- General arrangement of tunnel setup with outlet and flap installed. All dimensions are in inches.

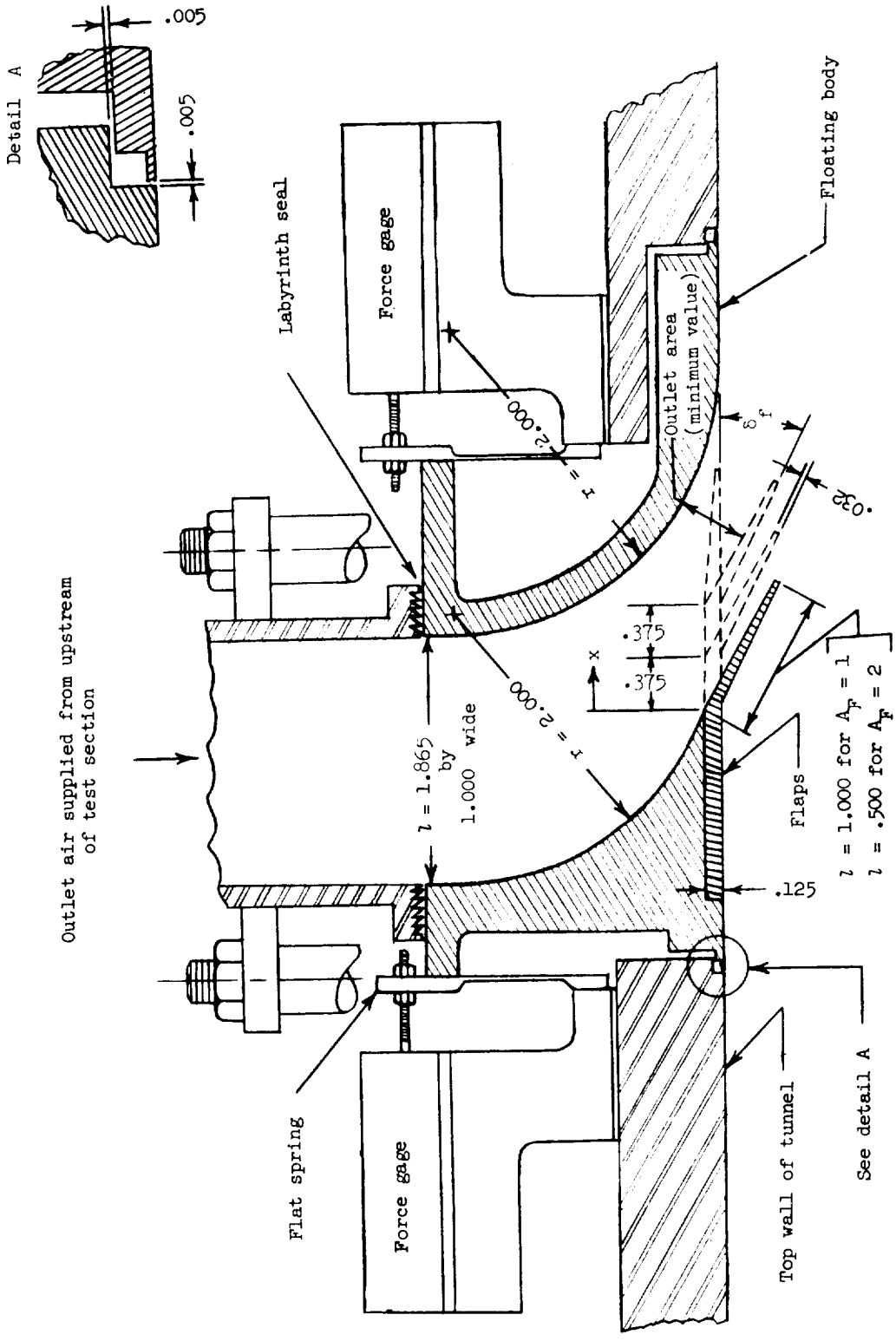

Figure 2.- Details of outlet and force balance. All dimensions are in inches.

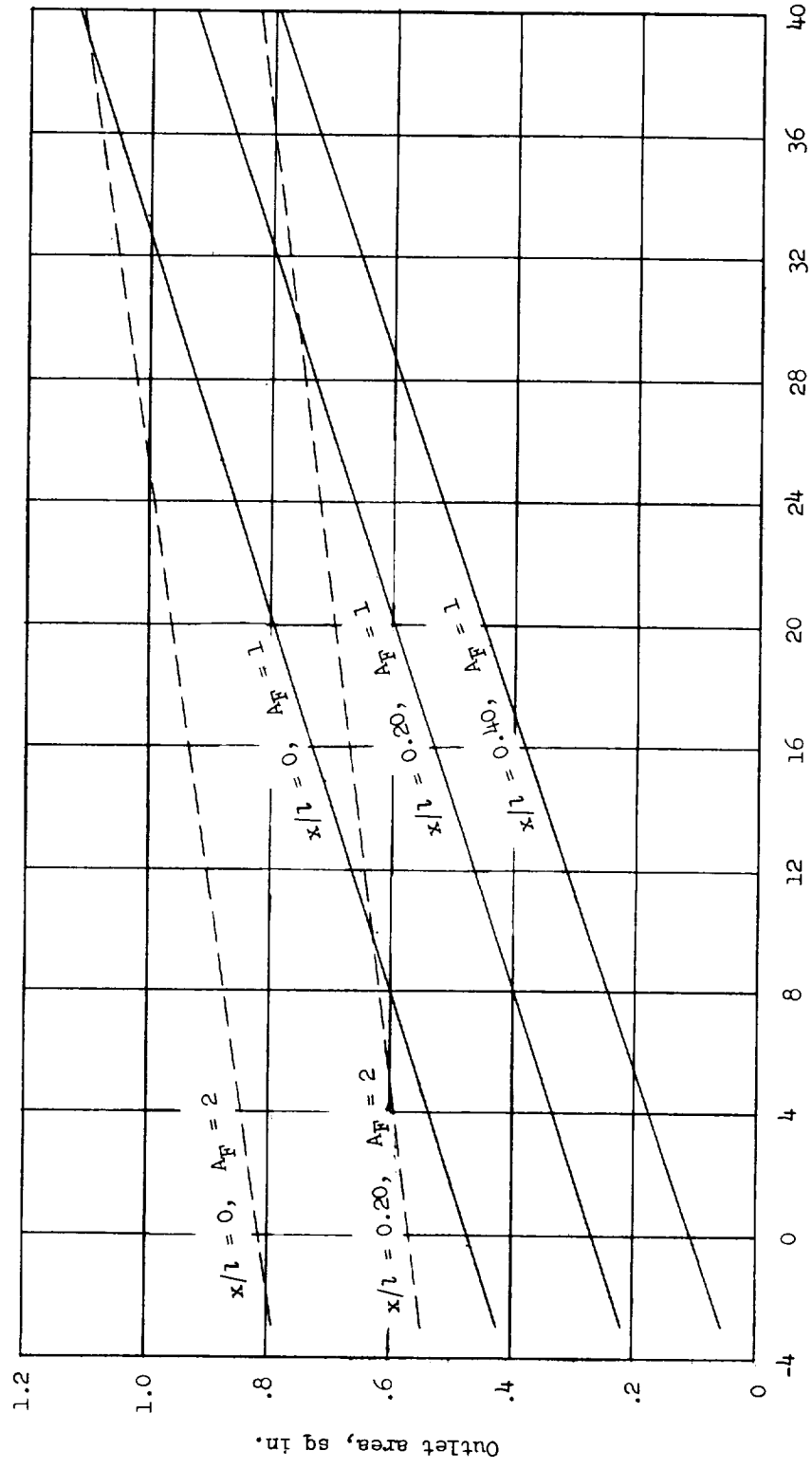

Figure 3.- Variation of outlet area with flap angle.

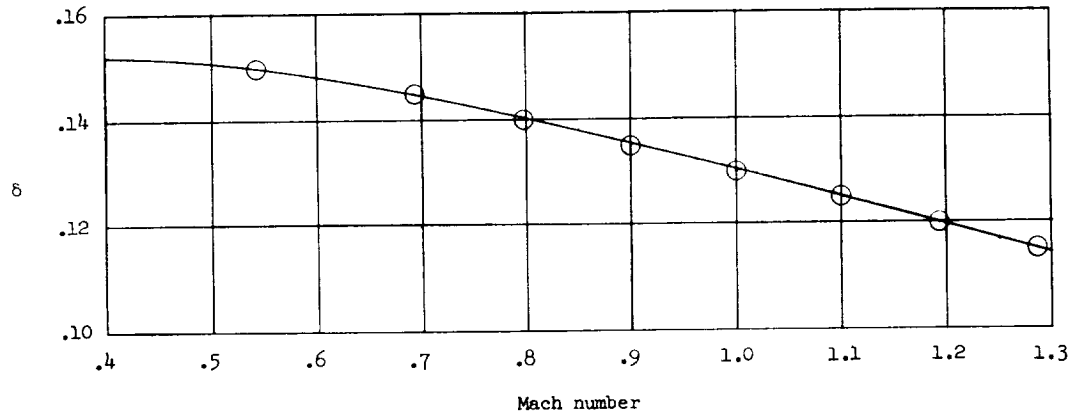

(a) Boundary-layer thickness.

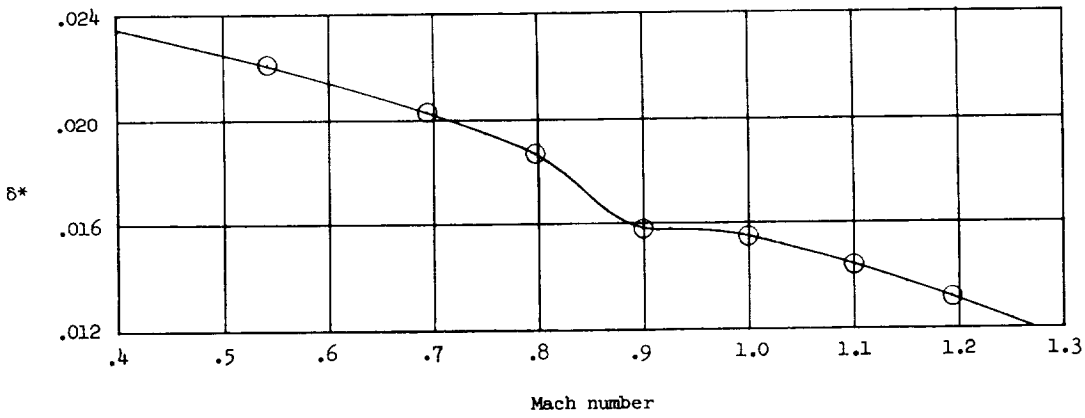

(b) Boundary-layer-displacement thickness.

Figure 4.- Variations of tunnel-wall boundary-layer parameters with stream Mach number.

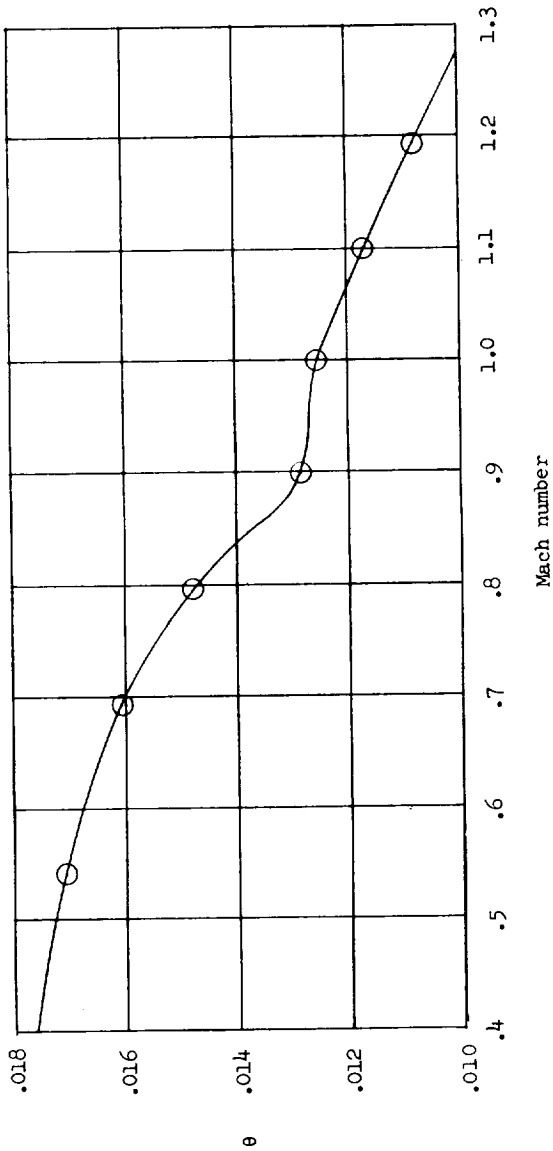

(c) Boundary-layer-momentum thickness.

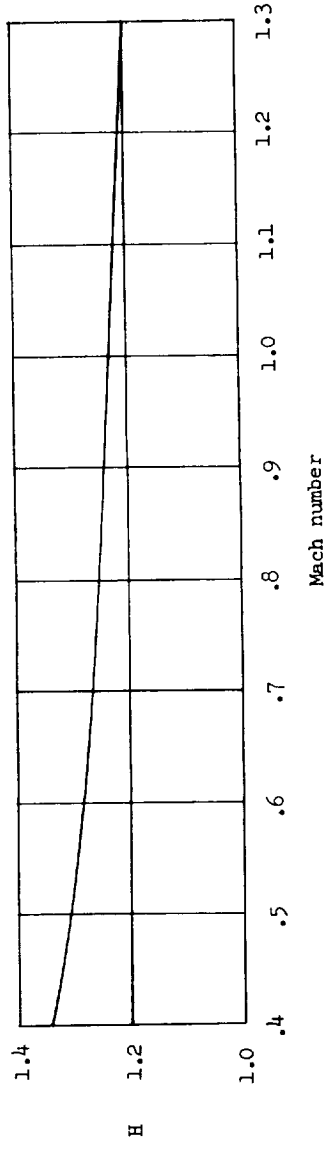

(d) Boundary-layer-shape parameter.

Figure 4.- Concluded.

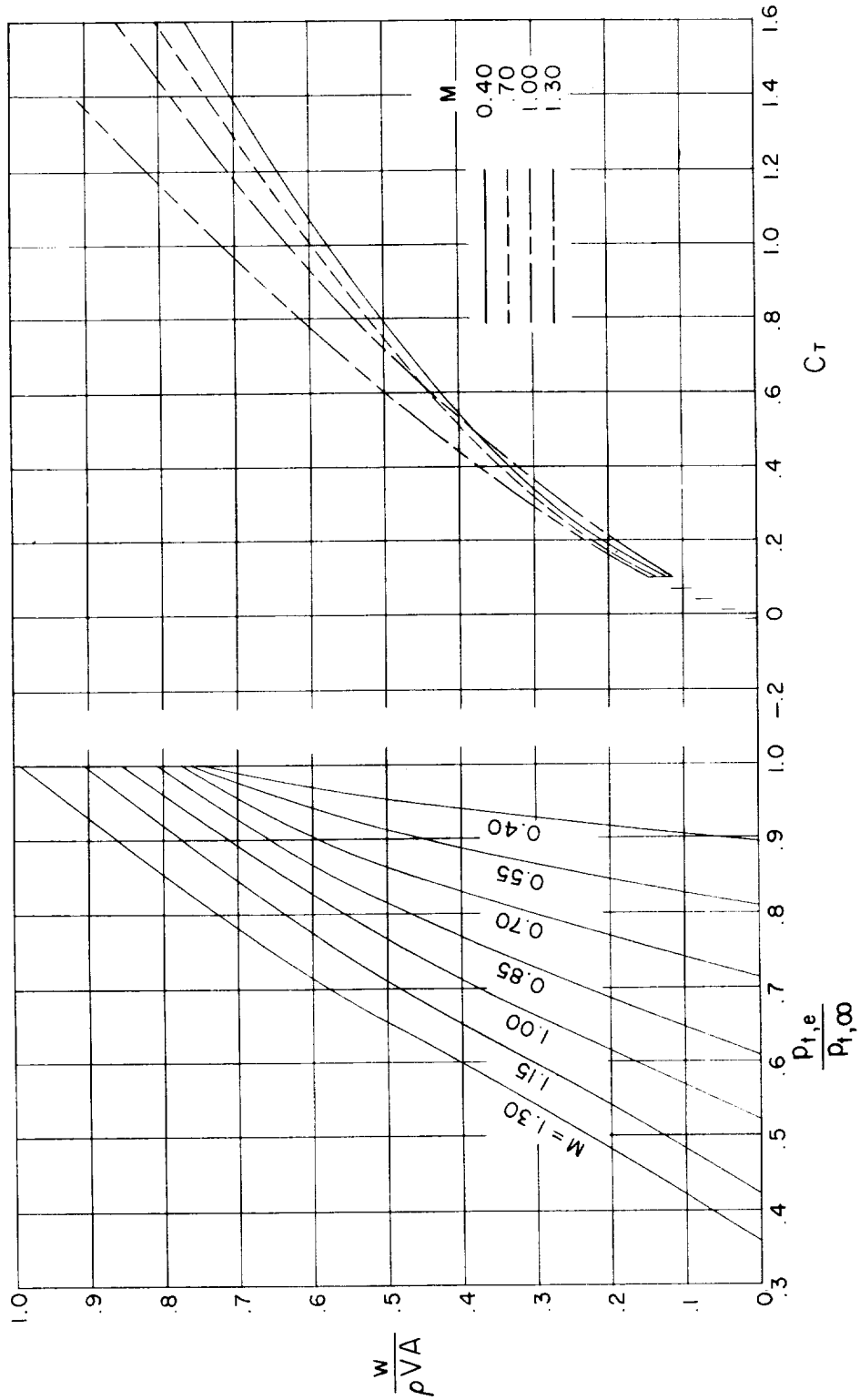

(a) $\delta_f = -0^\circ 21'$; $A_F = 1$; $x/l = 0$.

Figure 5.- Outlet discharge-flow ratio as a function of pressure ratio and of thrust coefficient.

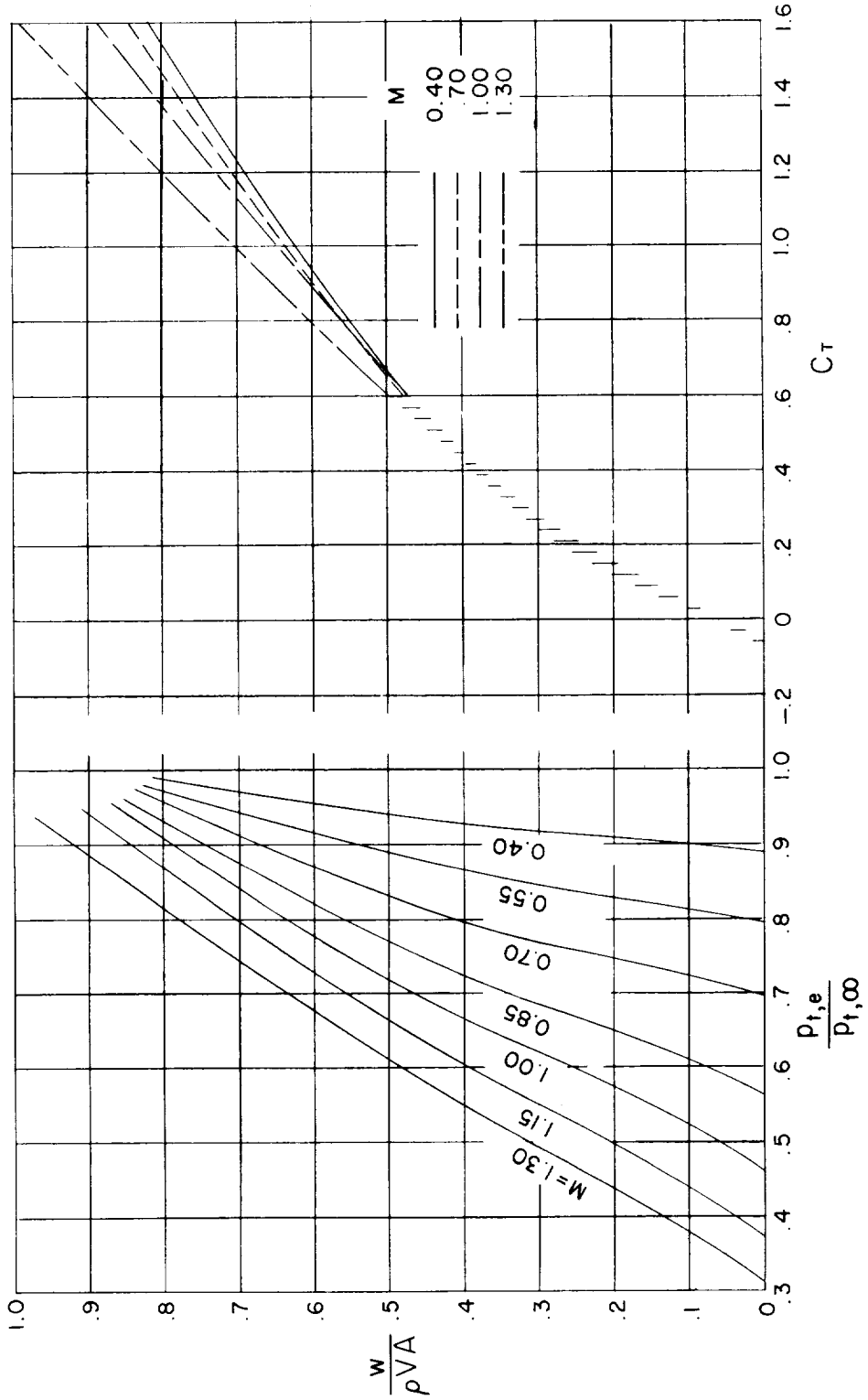

(b) $\delta_f = 4^\circ 41'$; $A_F = 1$; $x/l = 0$.

Figure 5.- Continued.

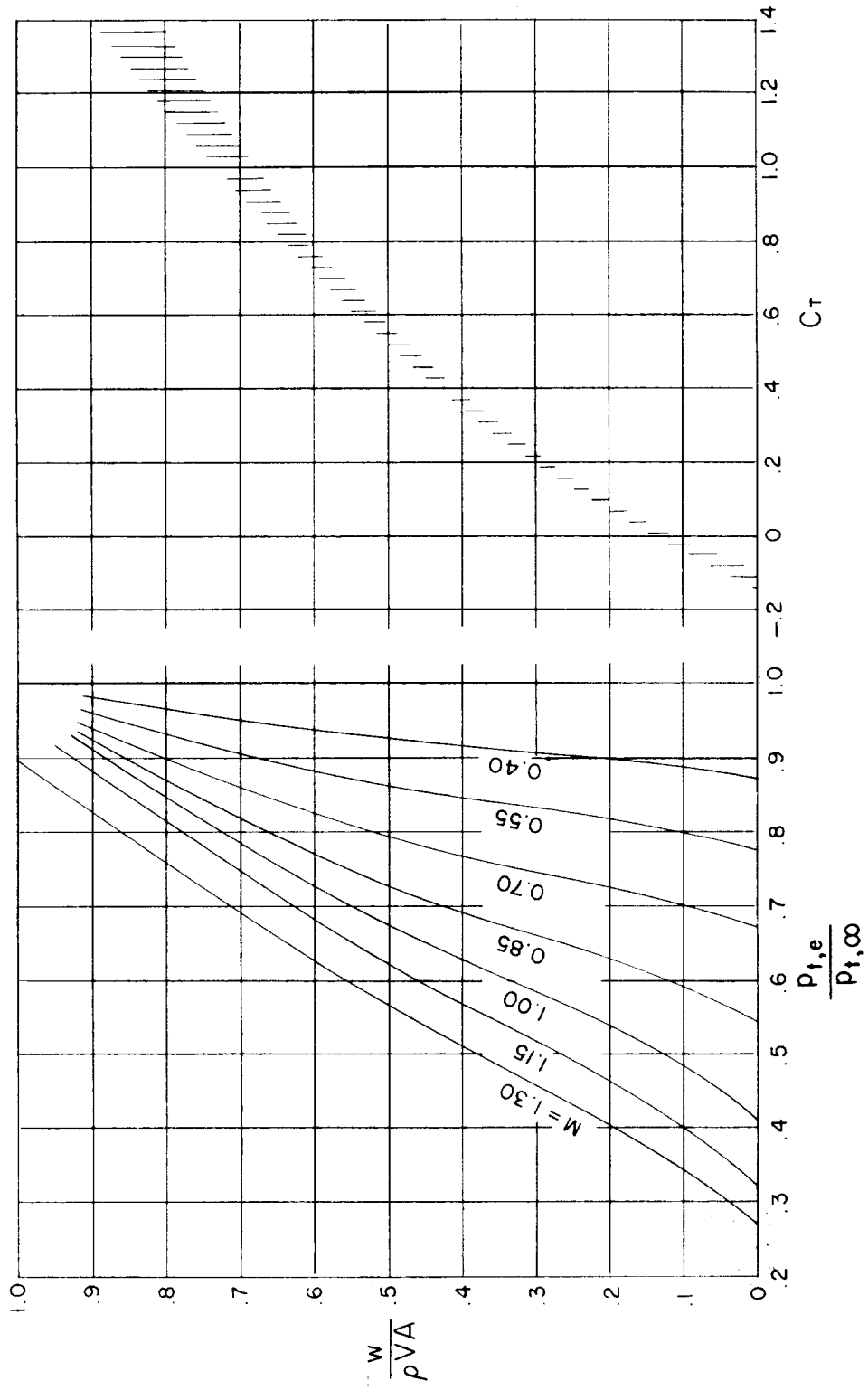

(c) $\delta_f = 9^\circ 46'$; $A_F = 1$; $x/l = 0$.

Figure 5.- Continued.

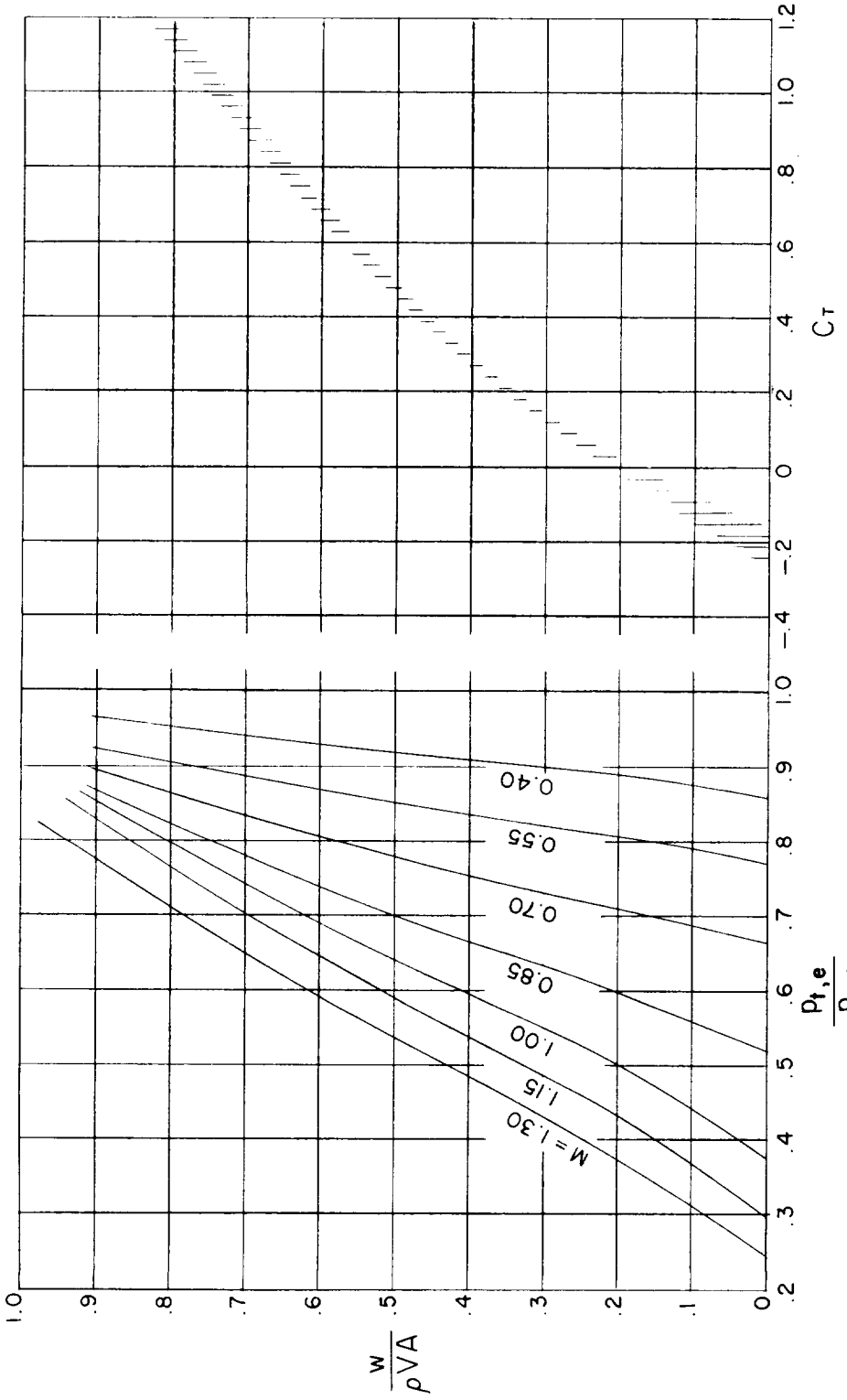

(d) $\delta_f = 14^\circ 54'$; $A_F = 1$; $x/l = 0$.

Figure 5.- Continued.

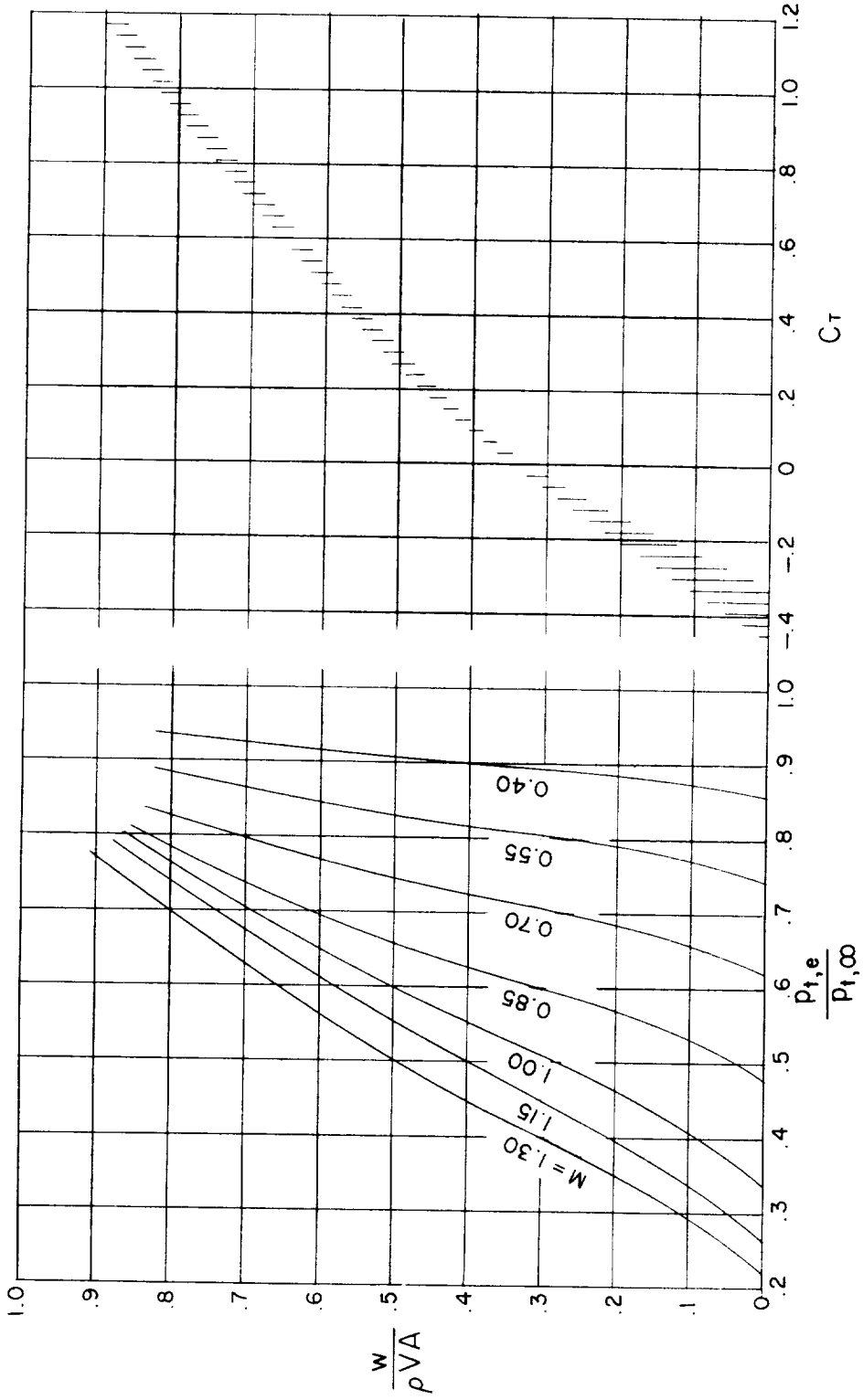

(e) $\delta_f = 25^\circ 21'$; $A_F = 1$; $x/l = 0$.

Figure 5.- Continued.

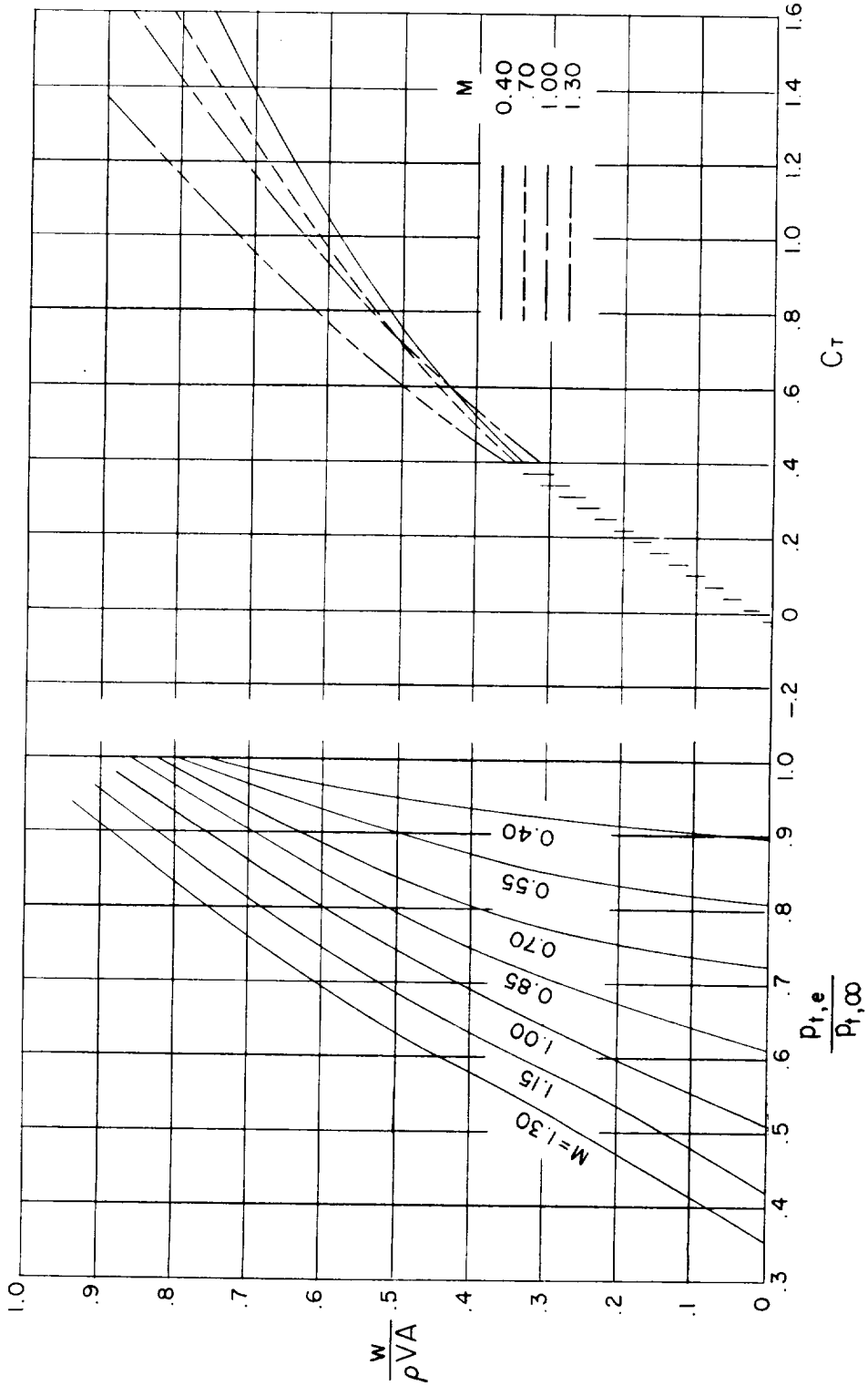

(f) $\delta_F = 0^\circ$; $A_F = 1$; $x/l = 0.20$.

Figure 5.- Continued.

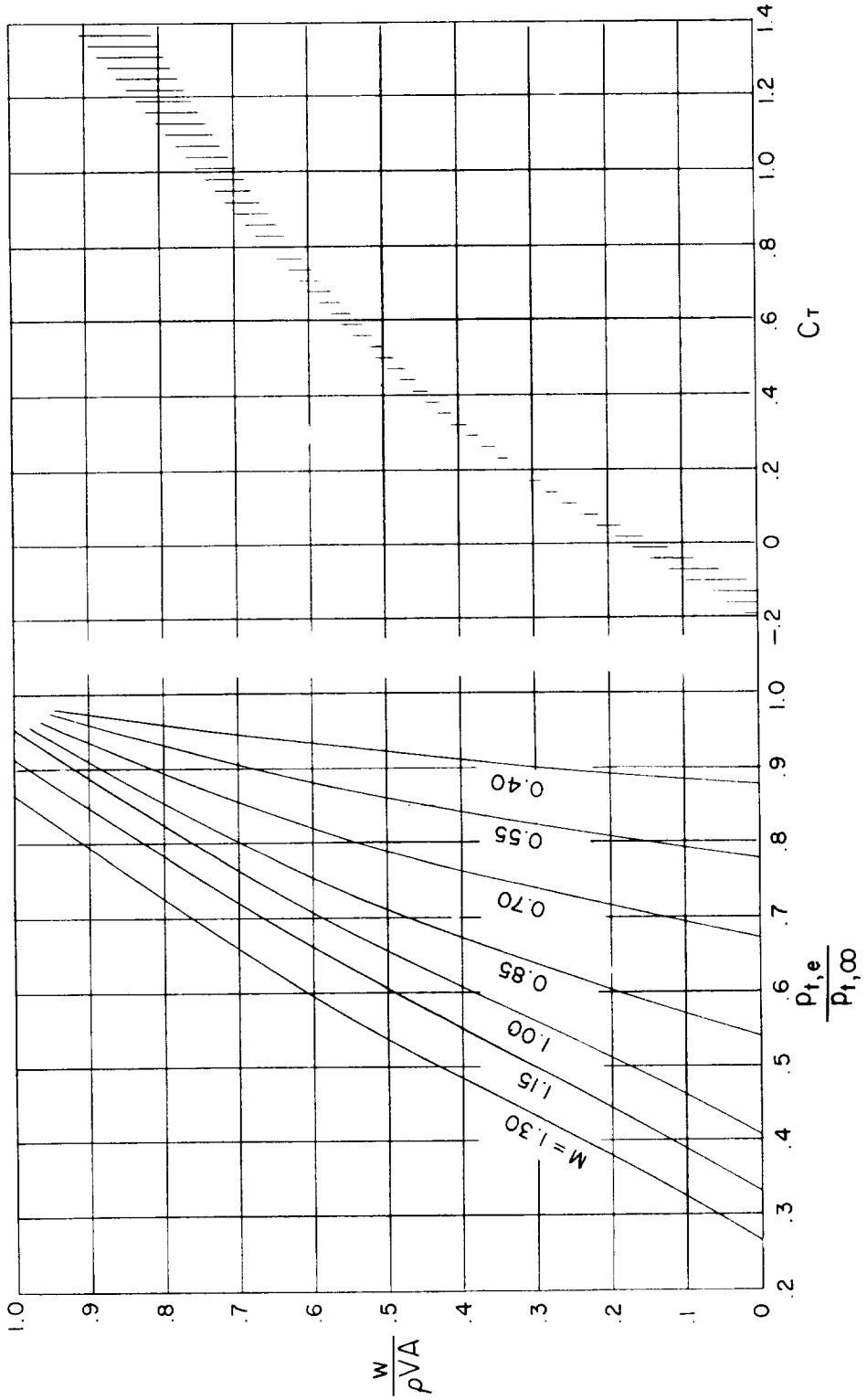

(g) $\delta_f = 9^\circ 46'$; $A_F = 1$; $x/l = 0.20$.

Figure 5.- Continued.

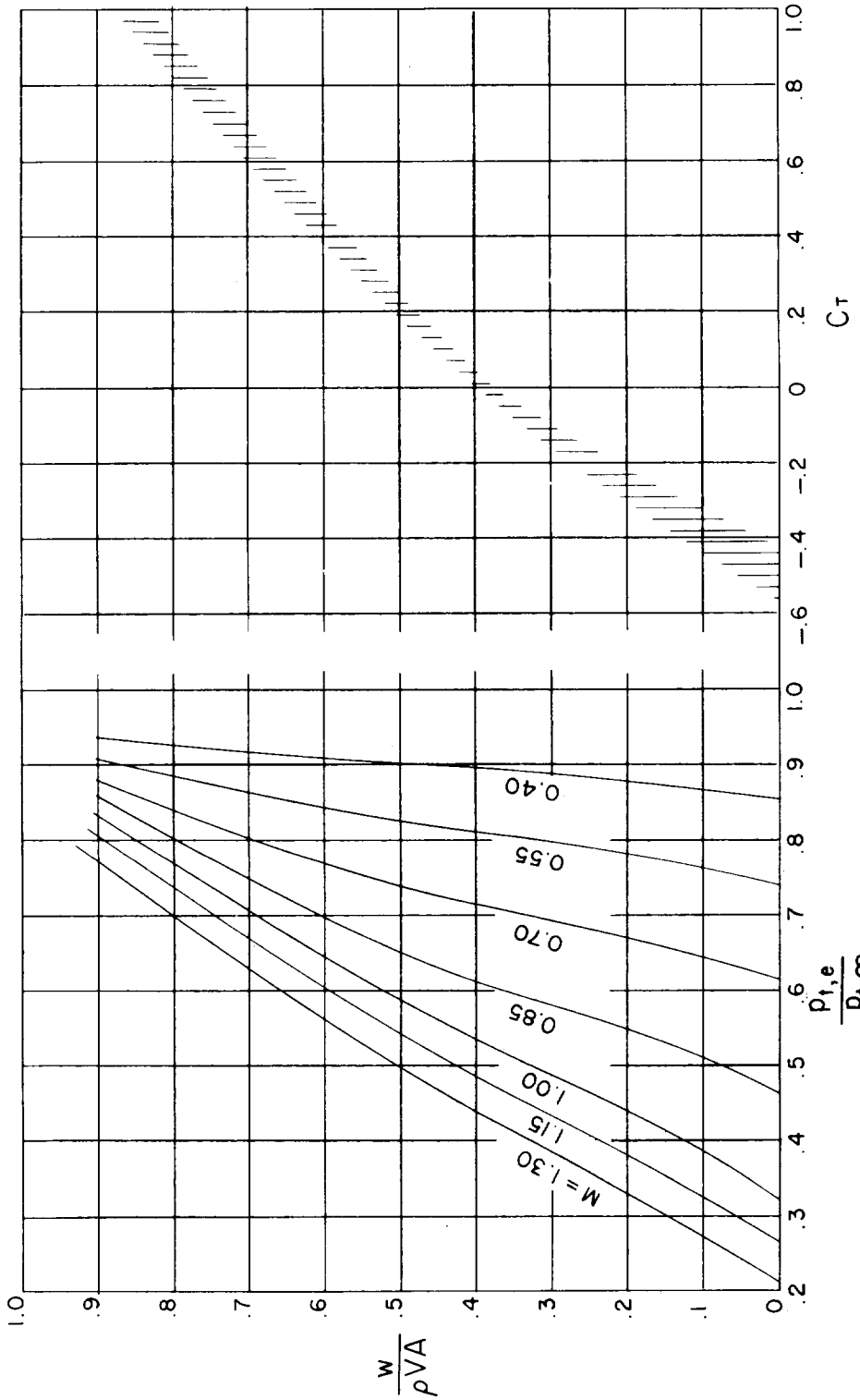

(h) $\delta_f = 25^\circ 21'$; $A_F = 1$; $x/l = 0.20$.

Figure 5.- Continued.

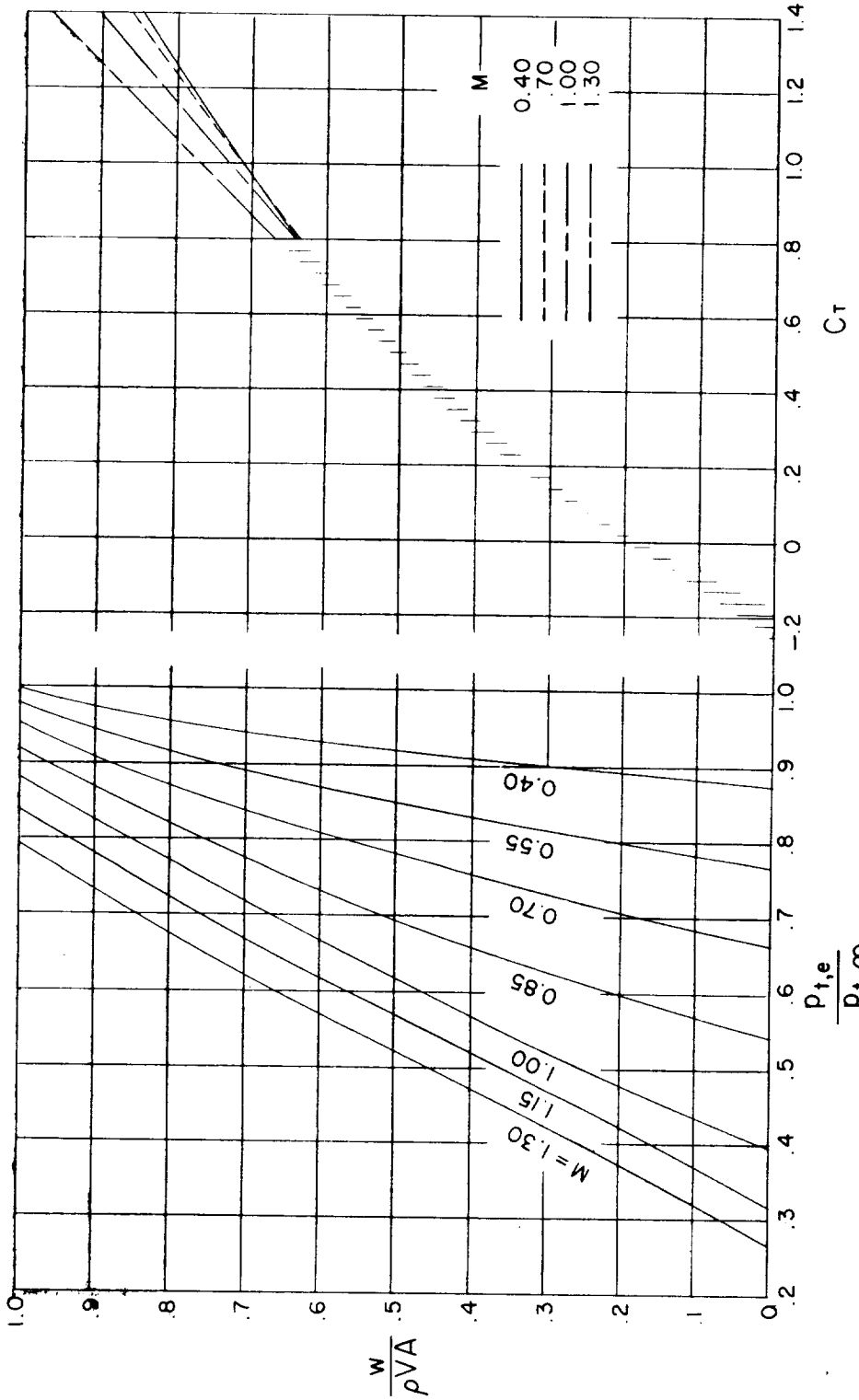

(i) $\delta_f = 9^\circ 46'$; $A_F = 1$; $x/l = 0.40$.

Figure 5.- Continued.

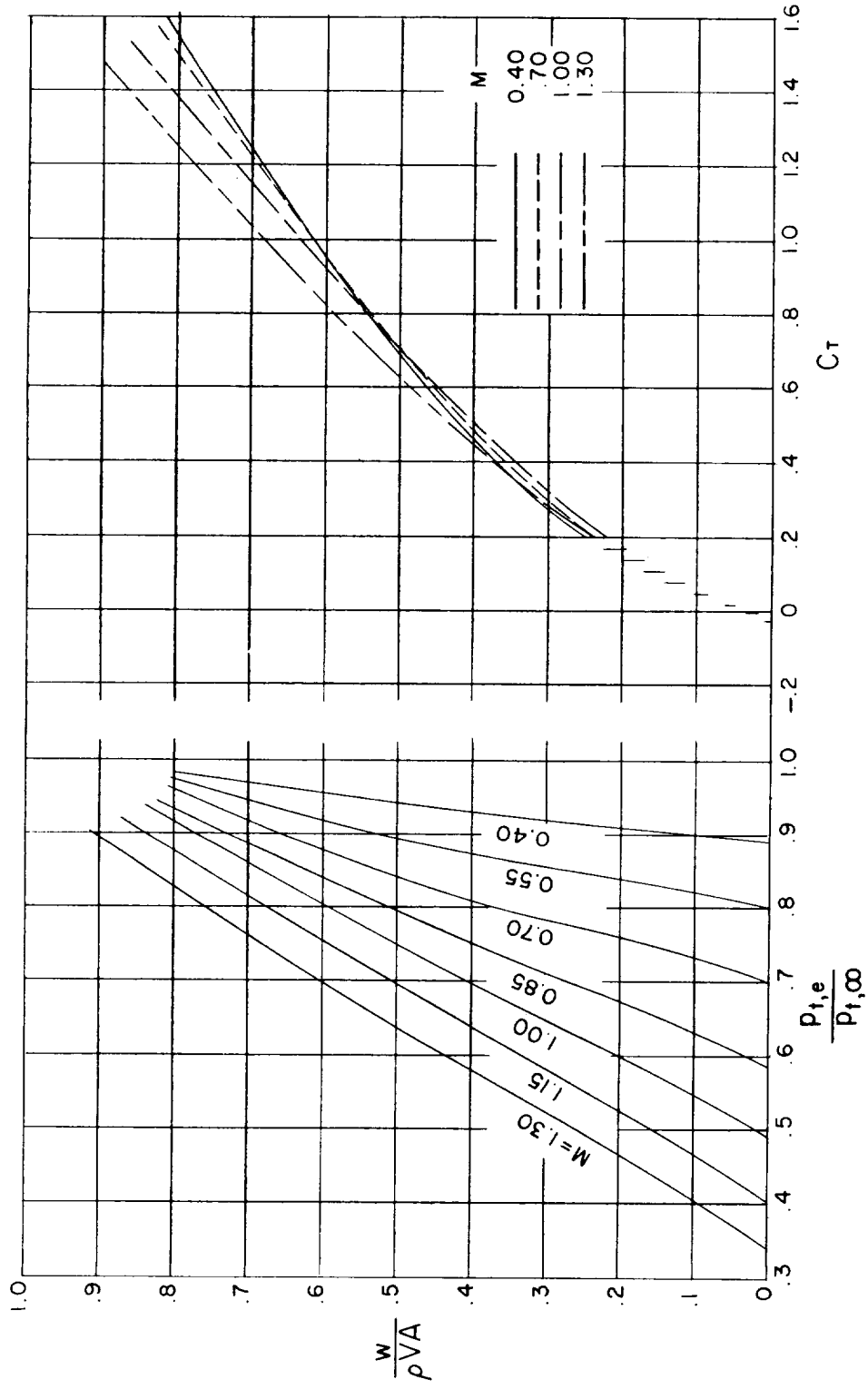

(j) $\delta_f = 4^\circ\ 15'$; $A_F = 2$; $x/l = 0$.

Figure 5.- Continued.

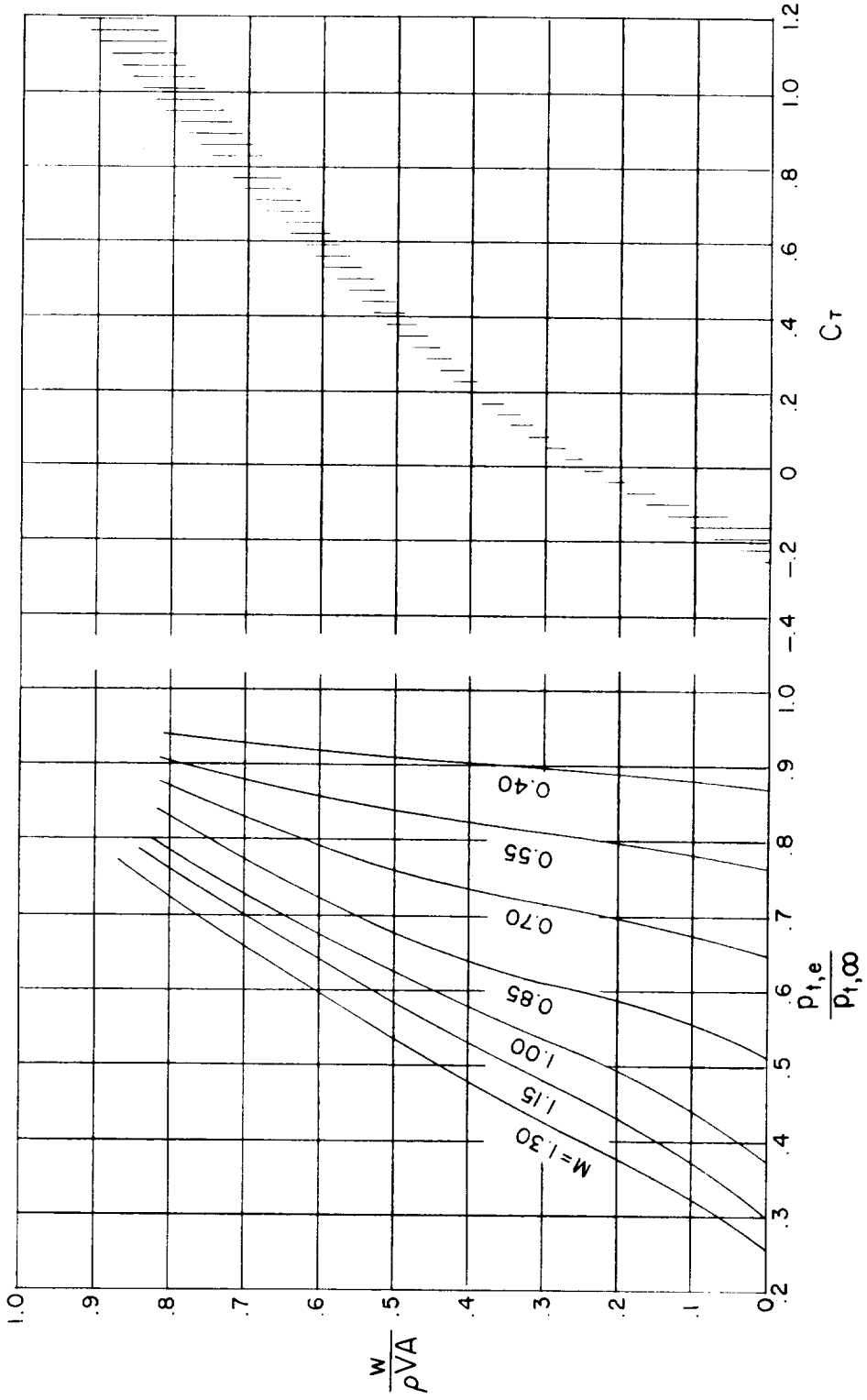

(k) $\delta_f = 37^\circ 12'$; $A_F = 2$; $x/l = 0$.

Figure 5.- Continued.

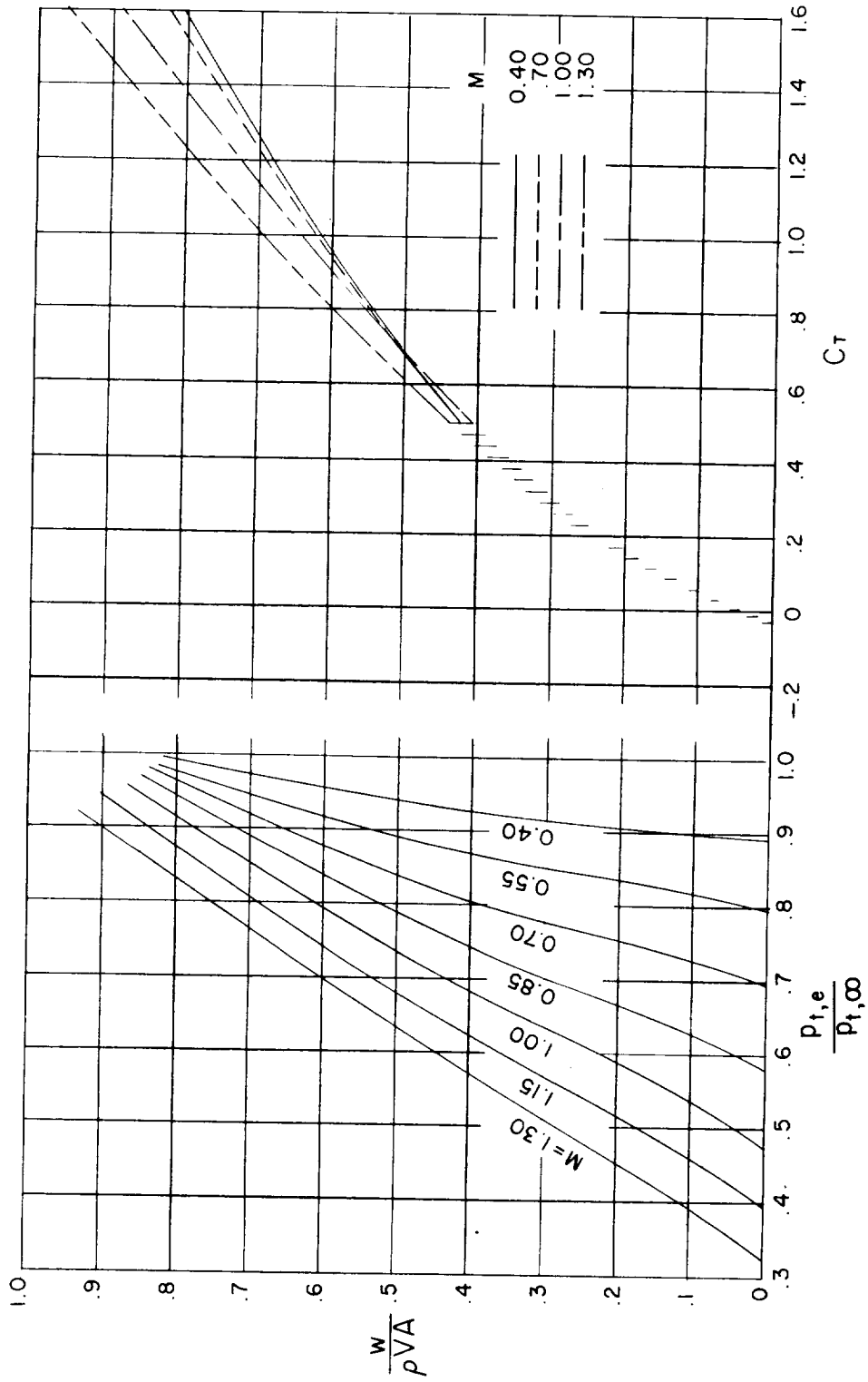

(l) $\delta_f = 40°\ 15'$; $A_F = 2$; $x/l = 0.20$.

Figure 5.- Continued.

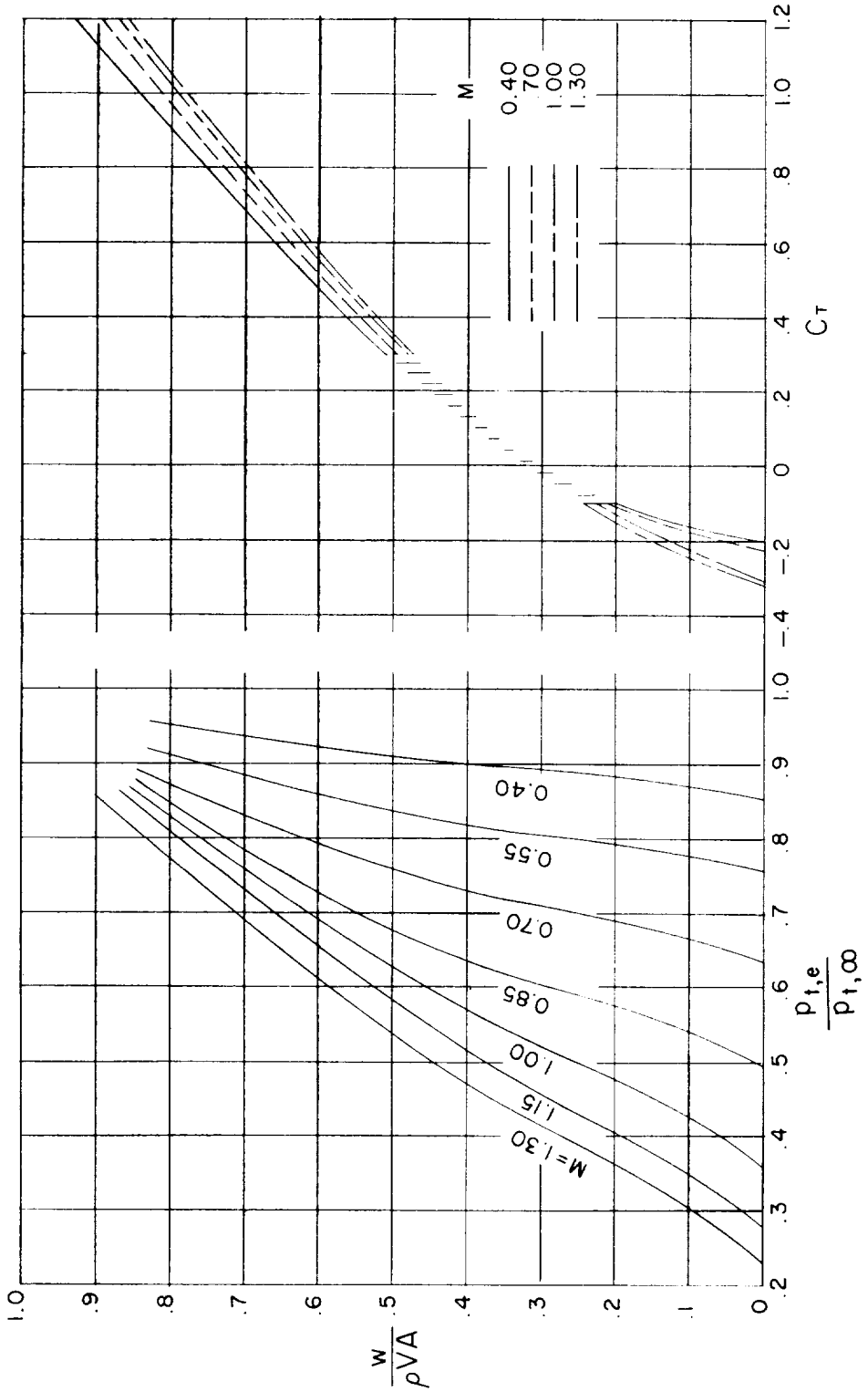

(m) $\delta_f = 37^\circ\ 12'$; $A_F = 2$; $x/l = 0.20$.

Figure 5.- Concluded.

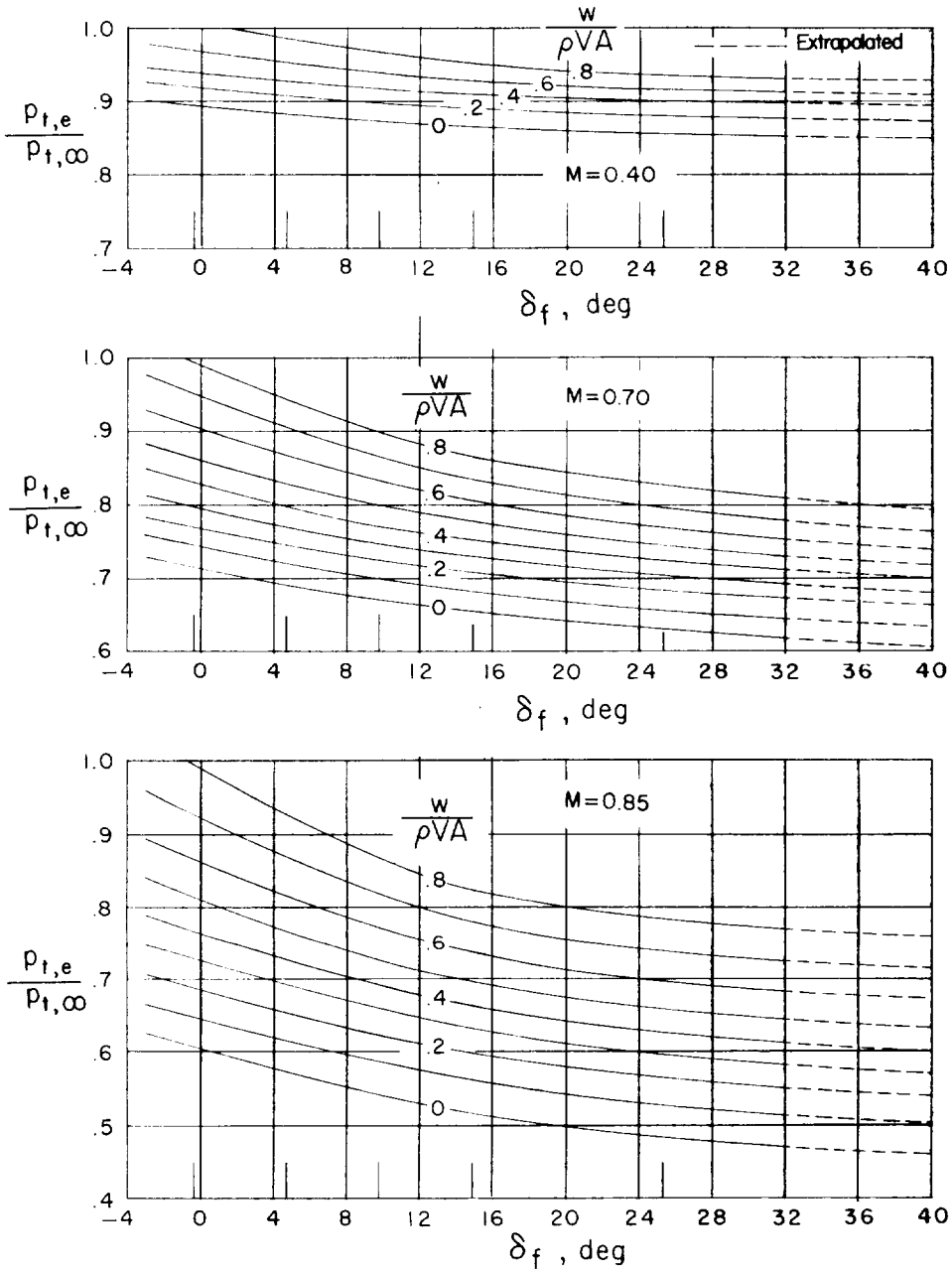

(a) $A_F = 1$; $x/l = 0$; M = 0.40, 0.70, and 0.85.

Figure 6.- Pressure ratio as a function of flap angle for varying outlet discharge-flow ratios. Bars along abscissa indicate flap angles tested.

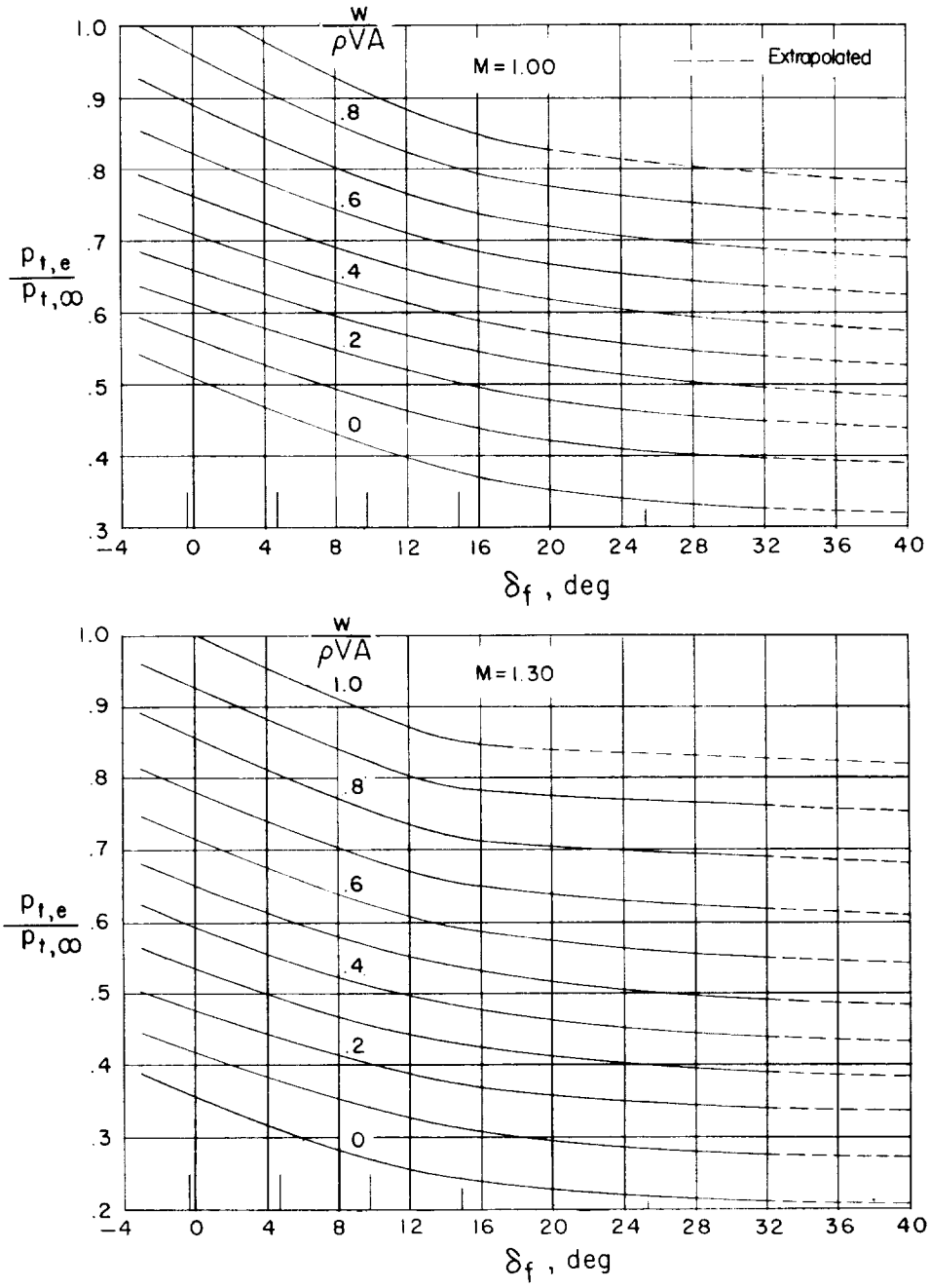

(b) $A_F = 1$; $x/l = 0$; M = 1.00 and 1.30.

Figure 6.- Continued.

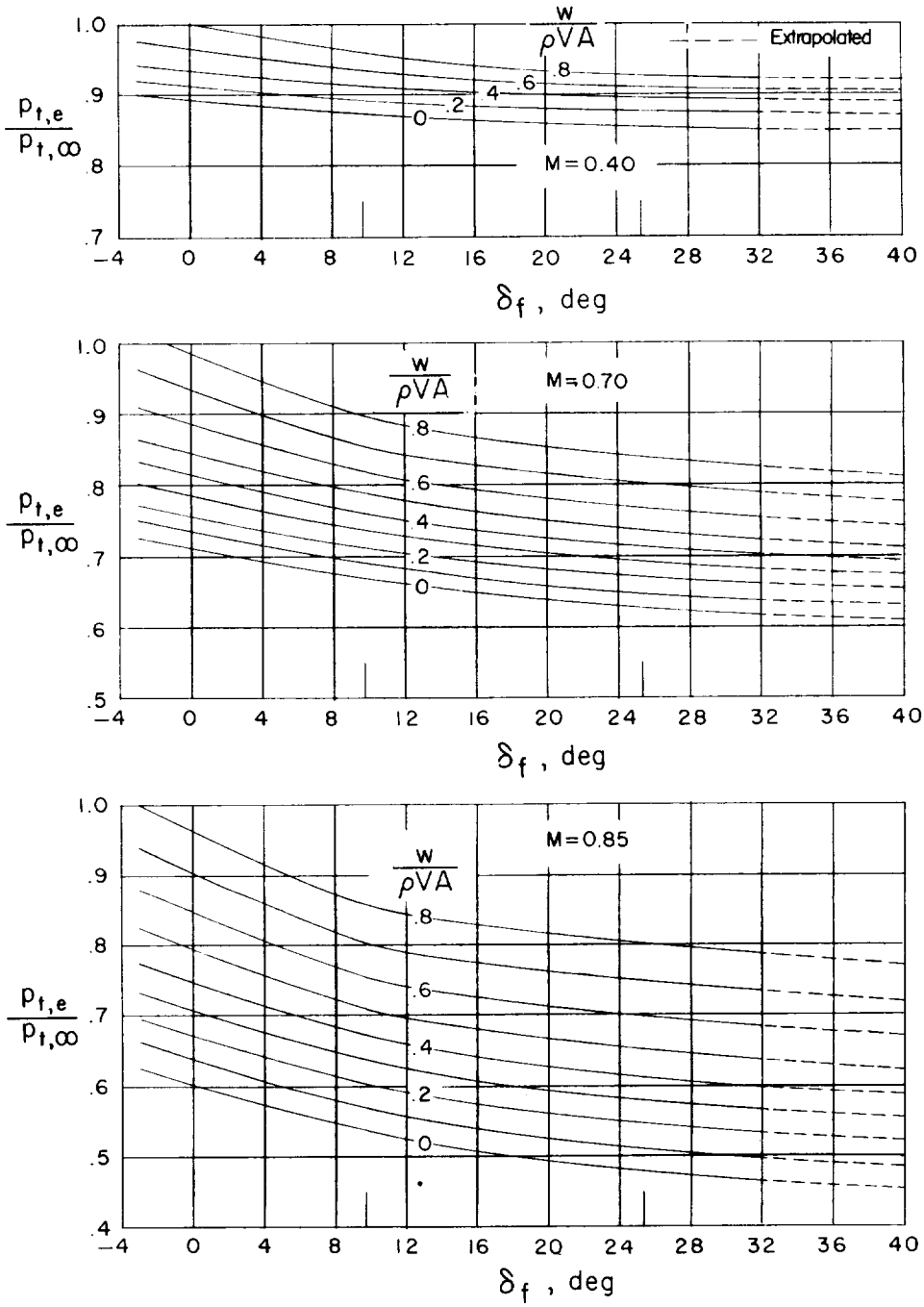

(c) $A_F = 1$; $x/l = 0.20$; M = 0.40, 0.70, and 0.85.

Figure 6.- Continued.

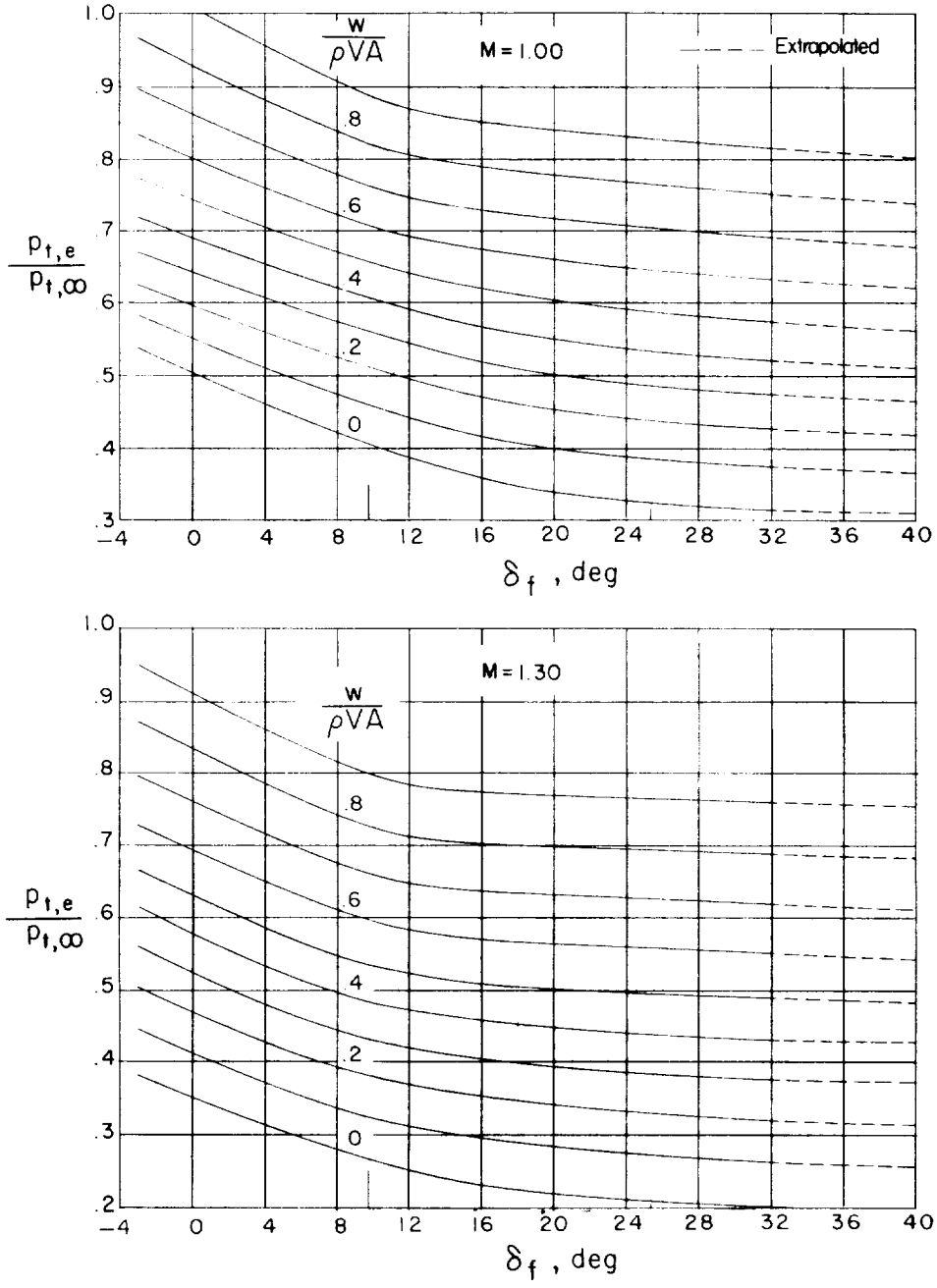

(d) $A_F = 1$; $x/l = 0.20$; M = 1.00 and 1.30.

Figure 6.- Continued.

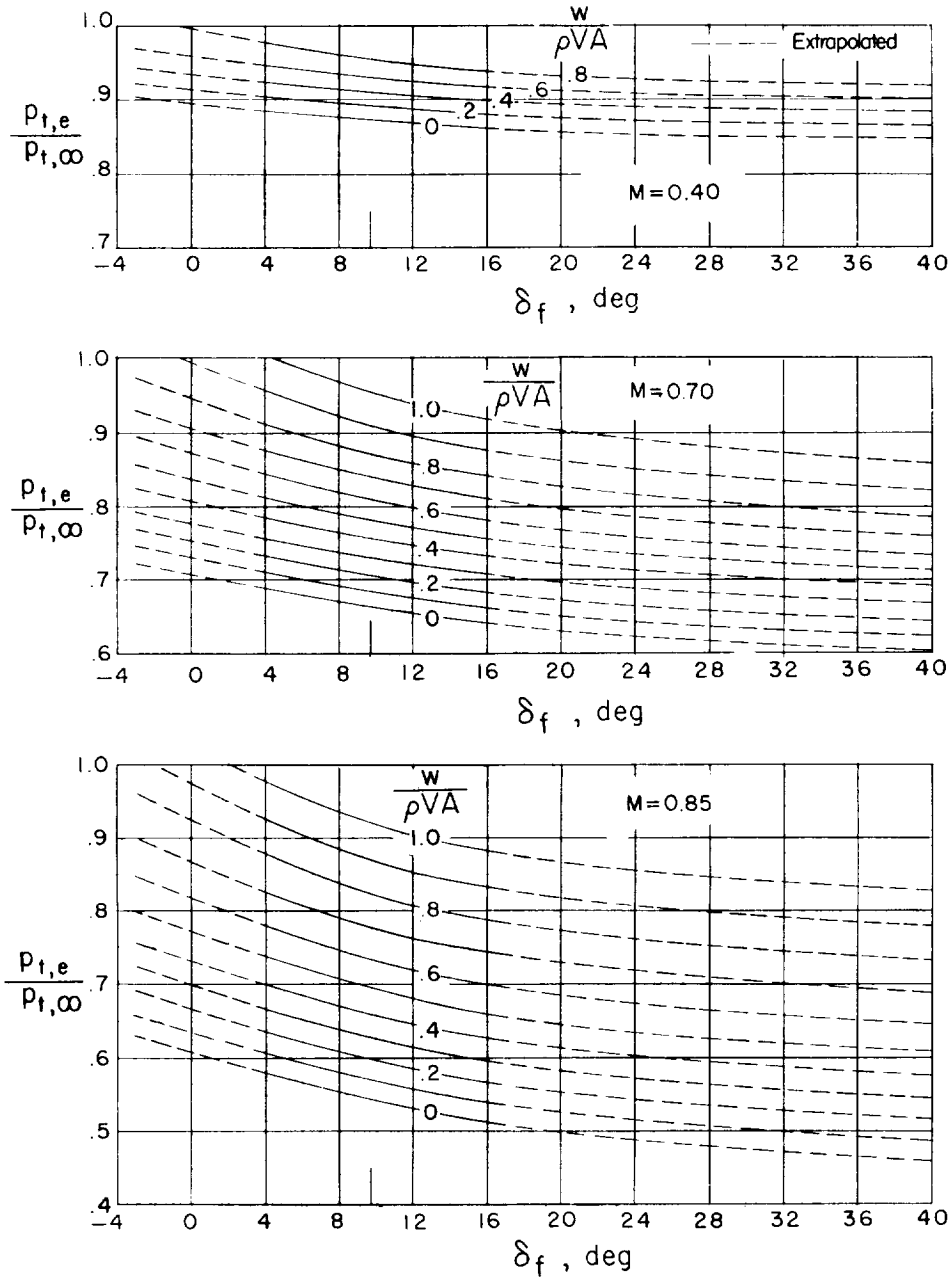

(e) $A_F = 1$; $x/l = 0.40$; M = 0.40, 0.70, and 0.85.

Figure 6.- Continued.

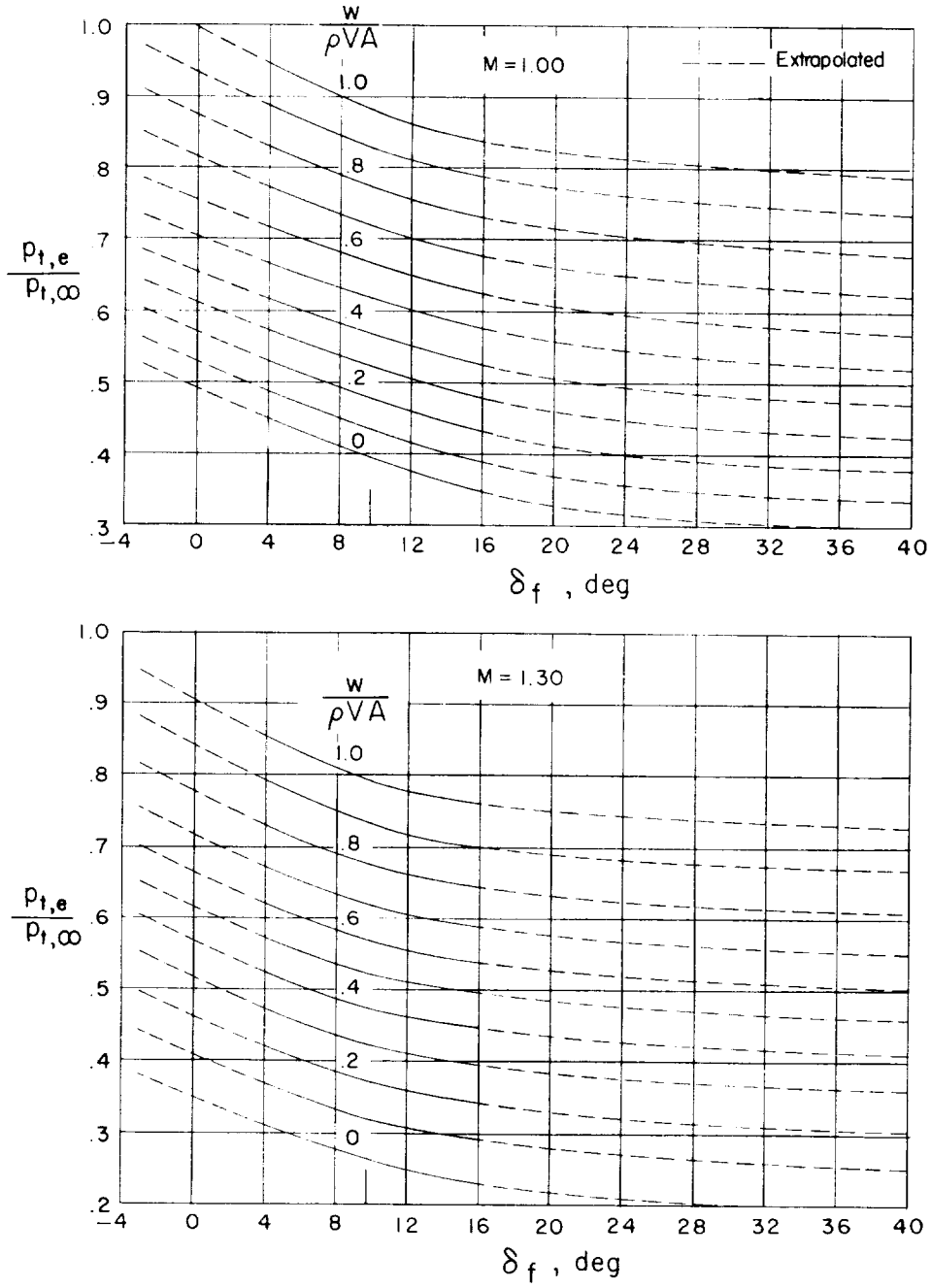

(f) $A_F = 1$; $x/l = 0.40$; M = 1.00 and 1.30.

Figure 6.- Continued.

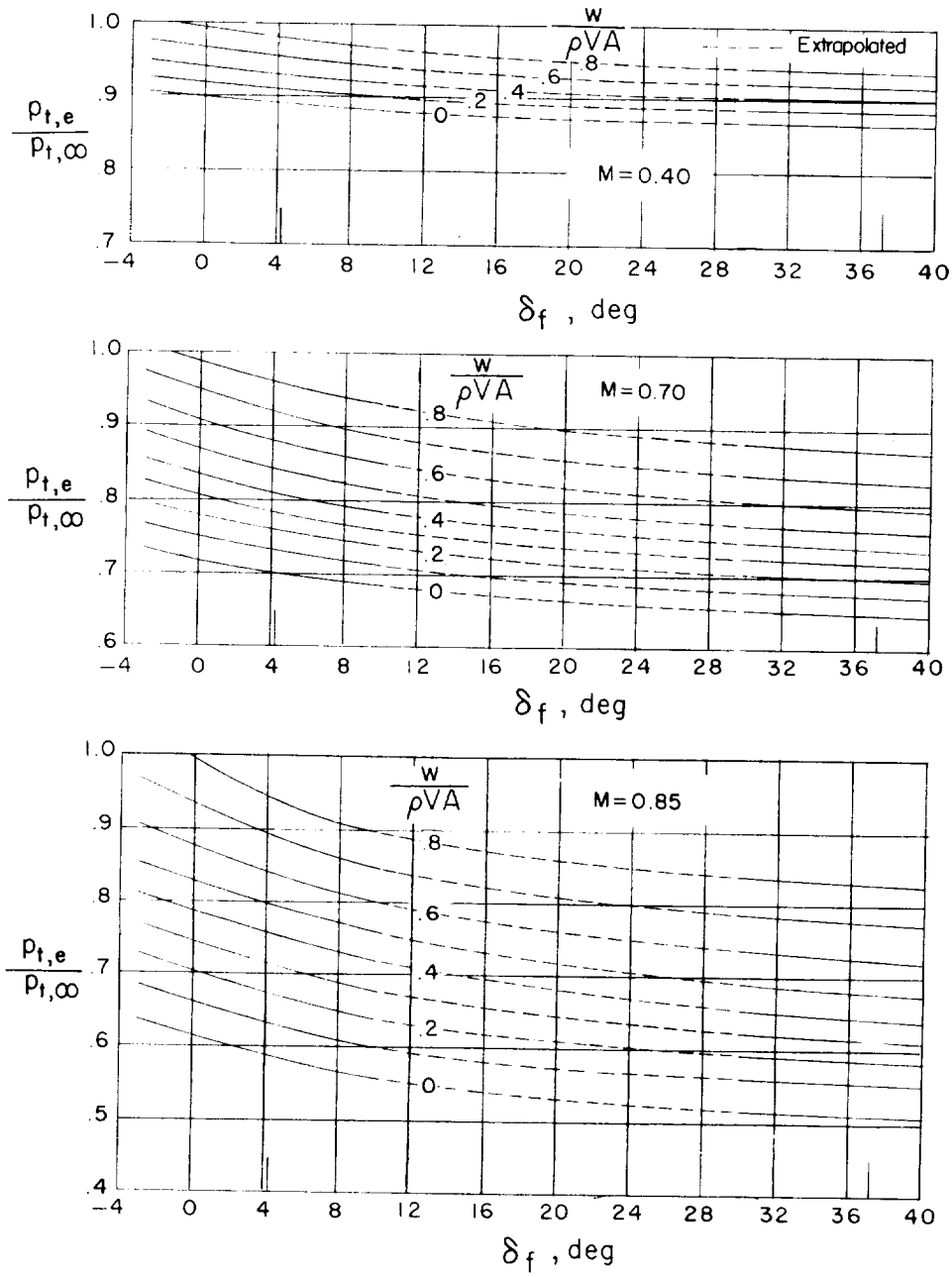

(g) $A_F = 2$; $x/l = 0$; M = 0.40, 0.70, and 0.85.

Figure 6.- Continued.

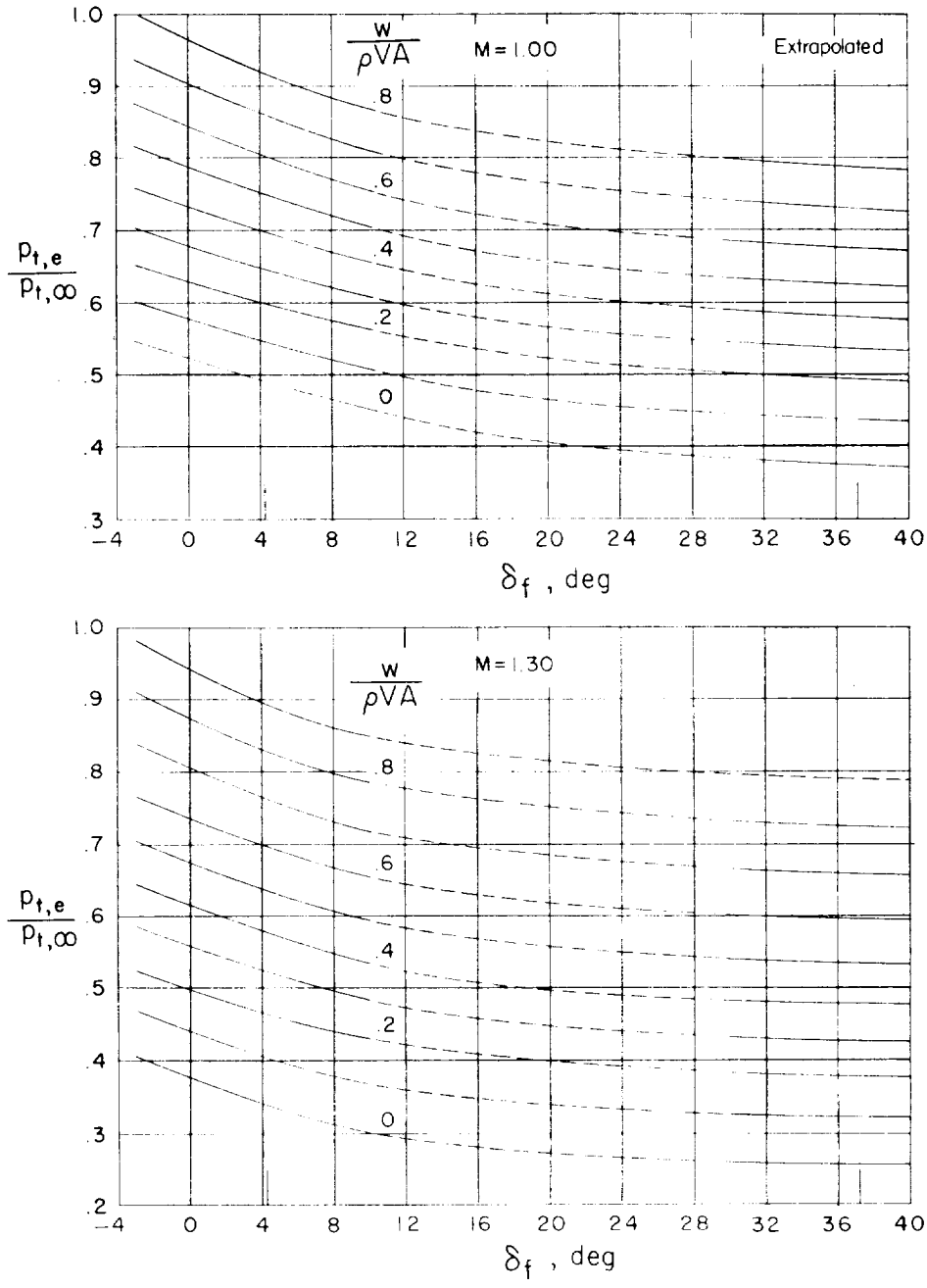

(h) $A_F = 2$; $x/l = 0$; M = 1.00 and 1.30.

Figure 6.- Continued.

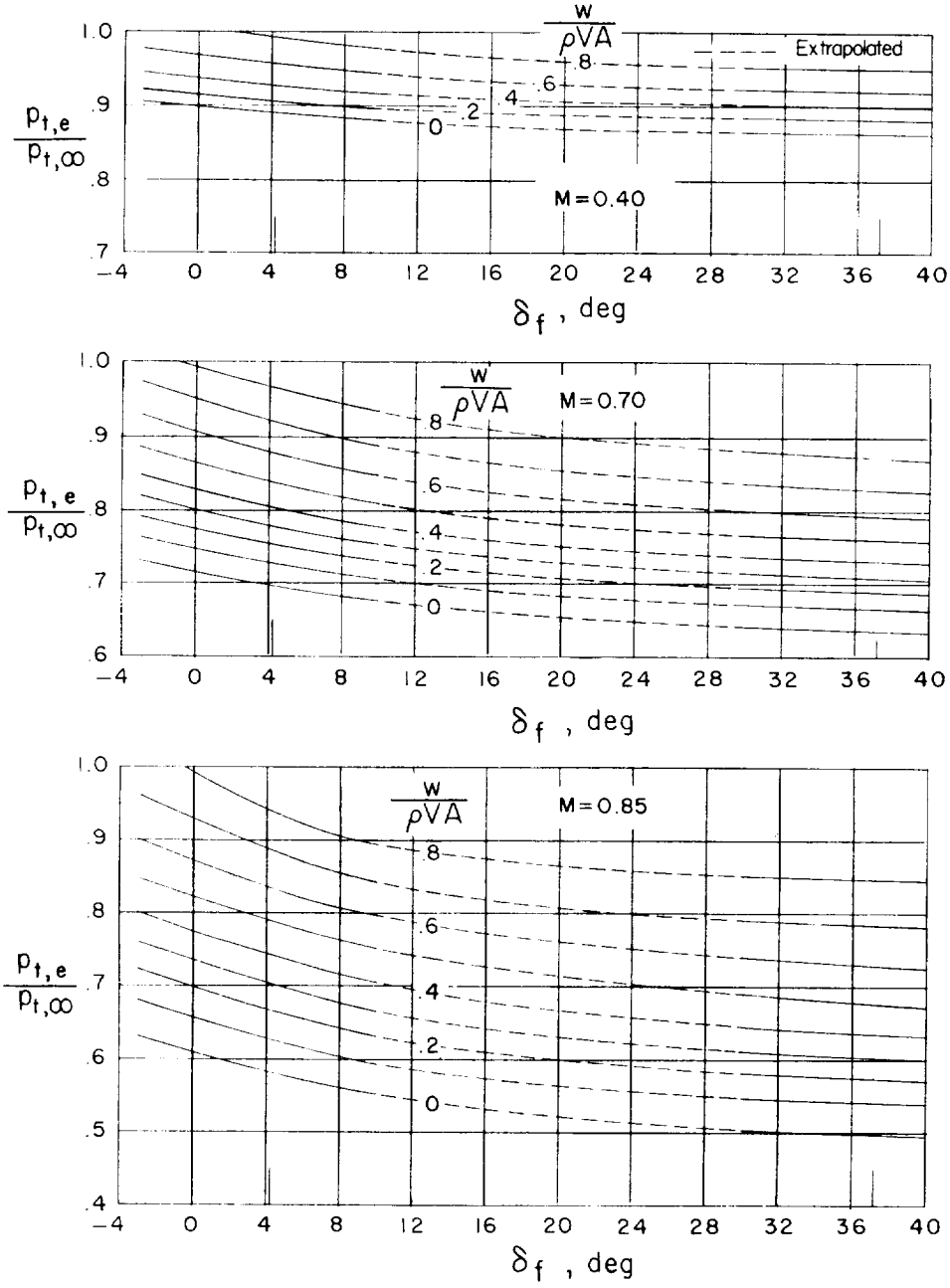

(i) $A_F = 2$; $x/l = 0.20$; M = 0.40, 0.70, and 0.85.

Figure 6.- Continued.

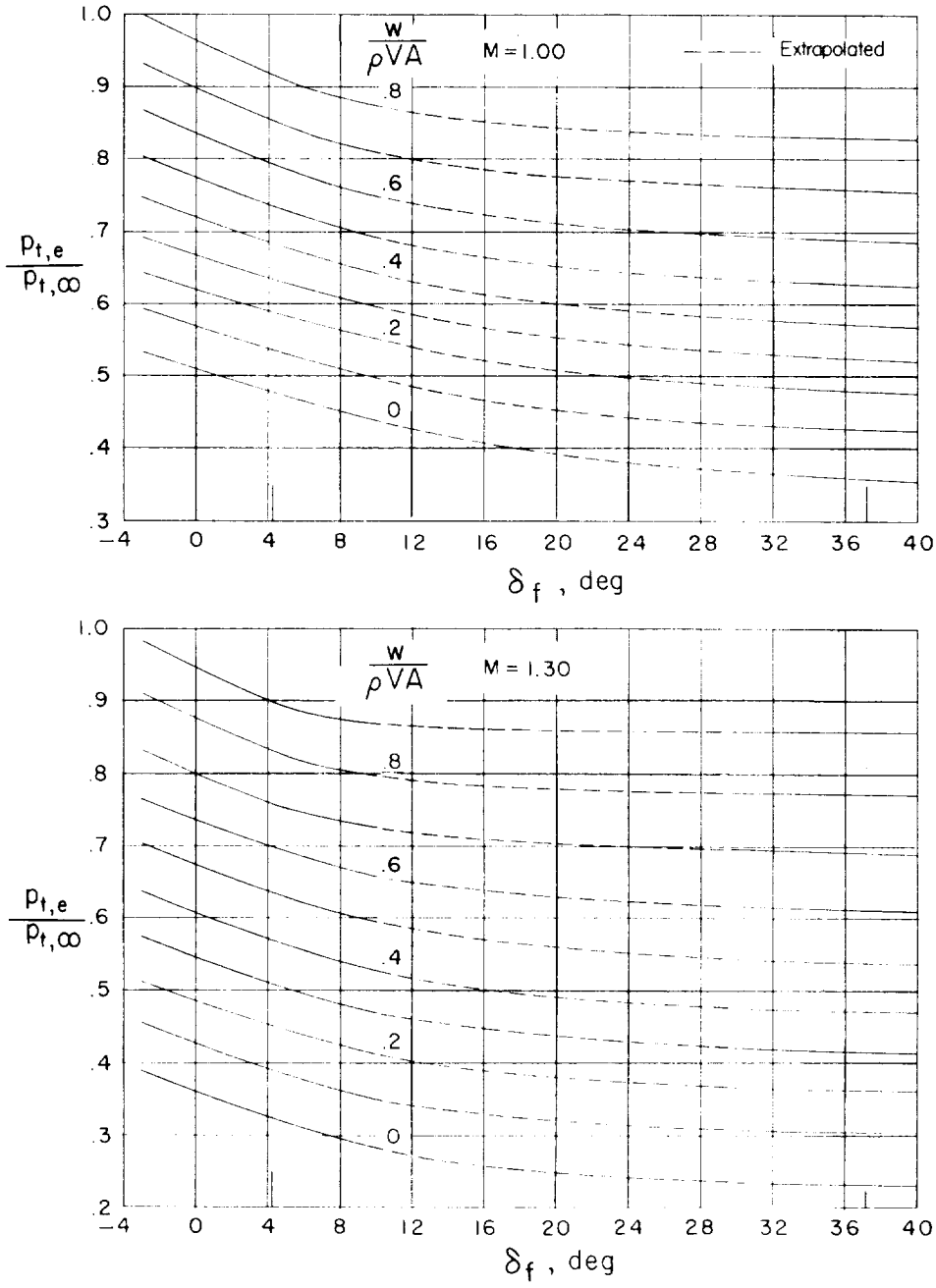

(j) $A_F = 2$; $x/l = 0.20$; M = 1.00 and 1.30.

Figure 6.- Concluded.

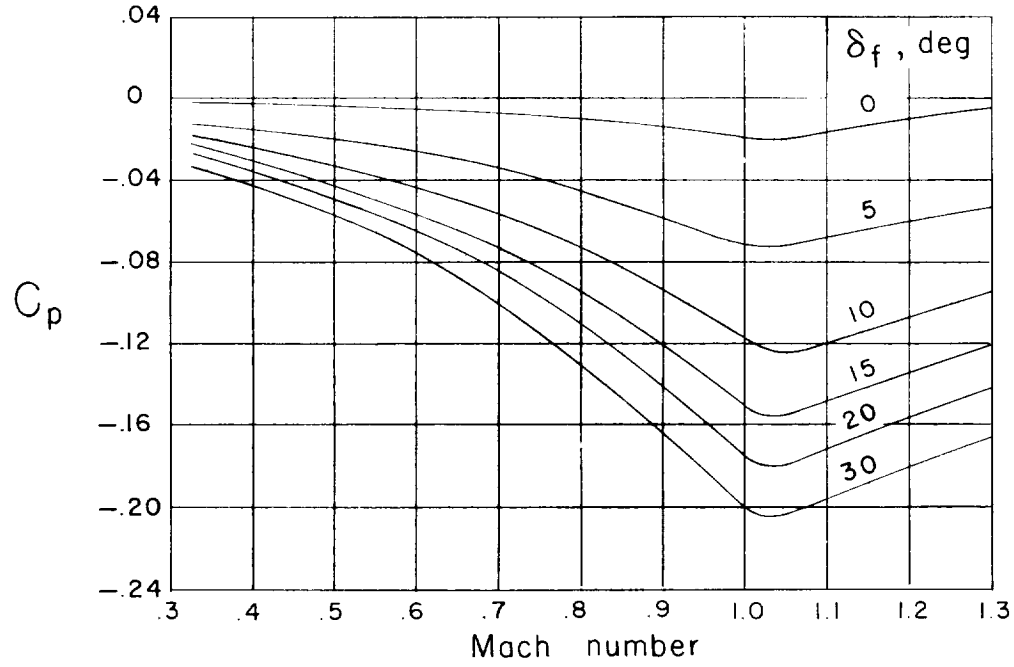

(a) $A_F = 1$; $x/l = 0$.

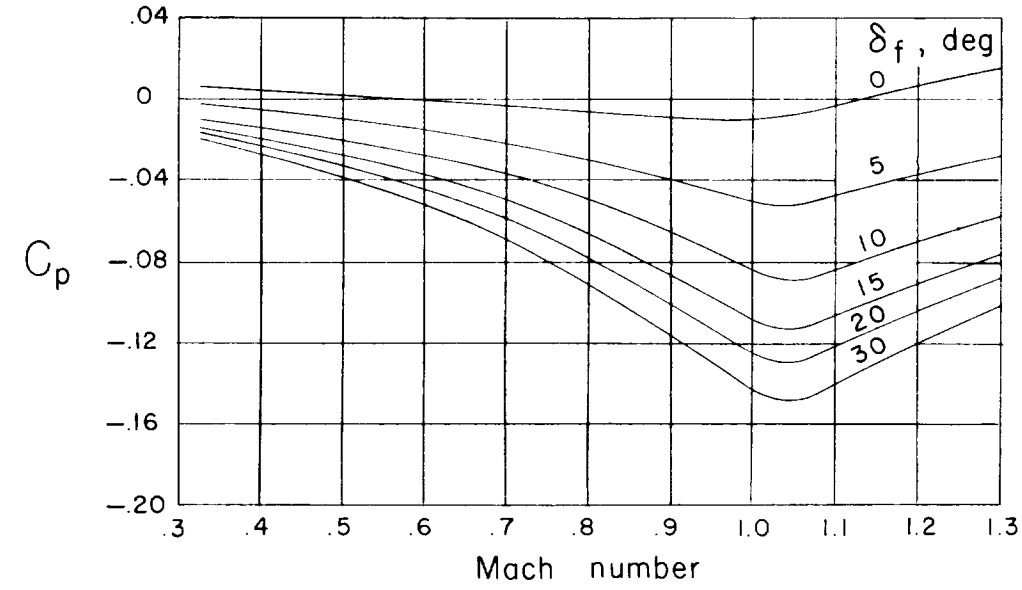

(b) $A_F = 2$; $x/l = 0$.

Figure 7.- Variations of vent pressure with Mach number at zero flow.

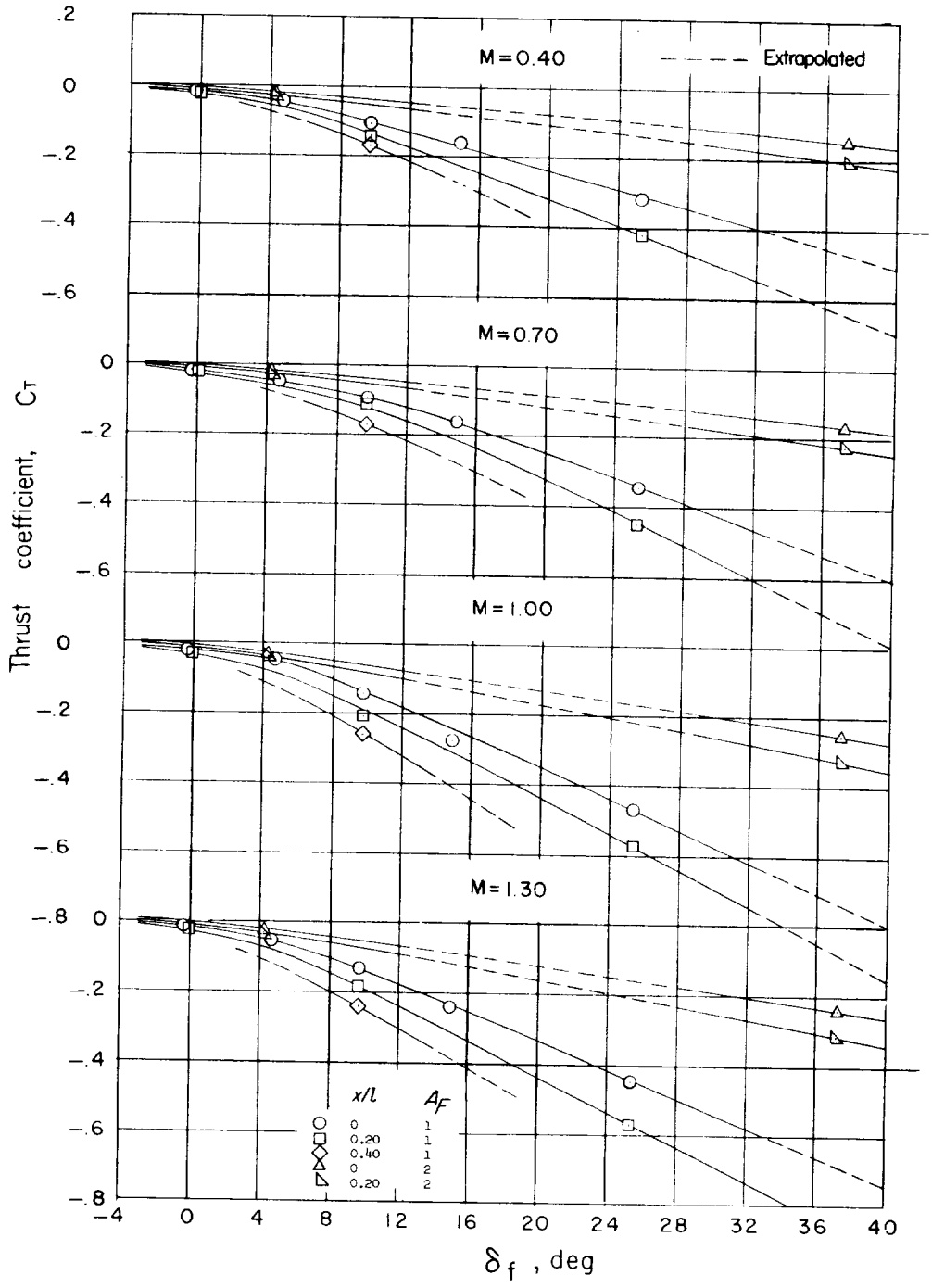

Figure 8.- Thrust coefficient as a function of flap angle for zero discharge-flow rate. $\frac{W}{\rho VA} = 0$.

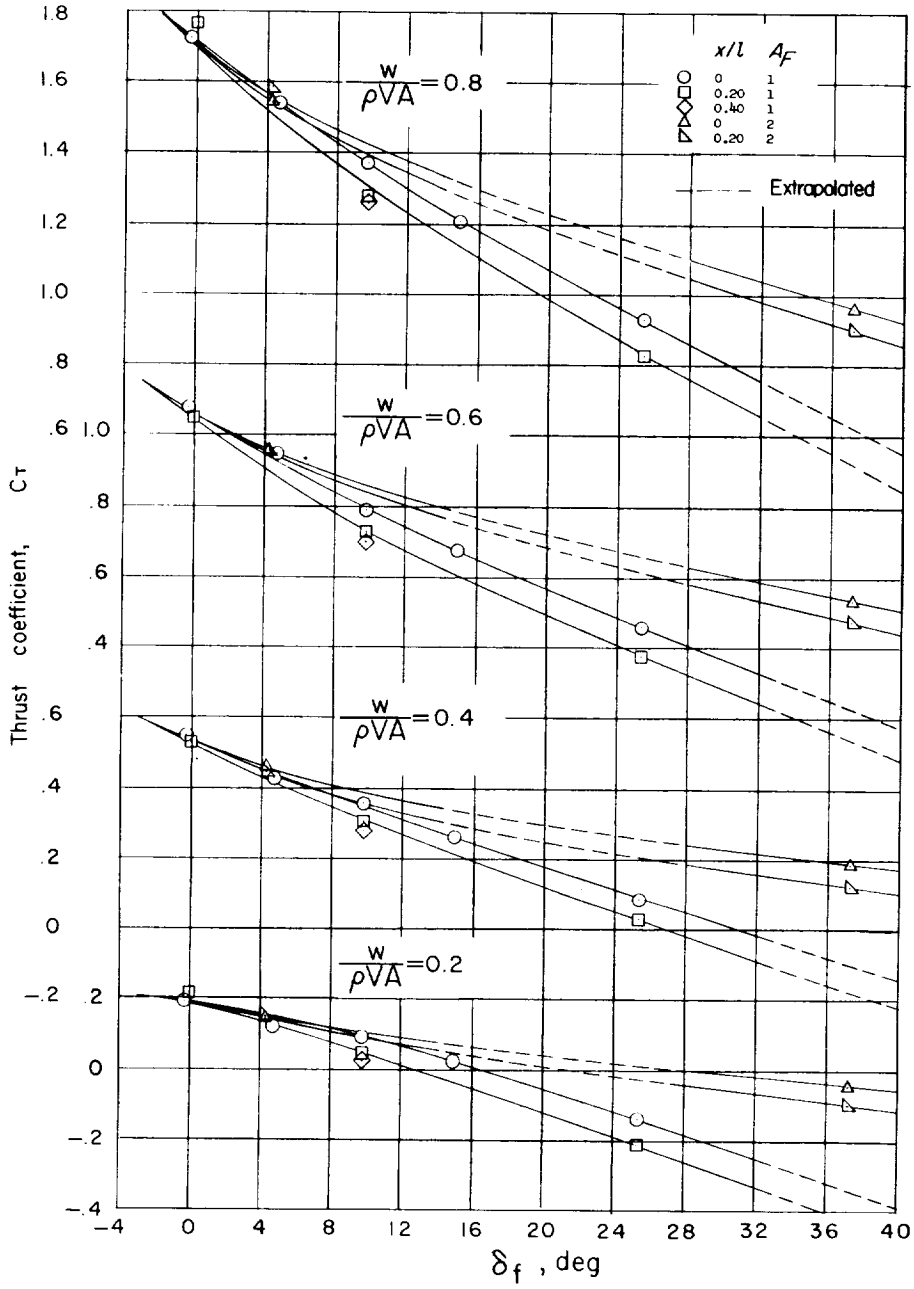

(a) Mach number = 0.40.

Figure 9.- Design charts of thrust coefficient as a function of flap angle for various discharge-flow ratios.

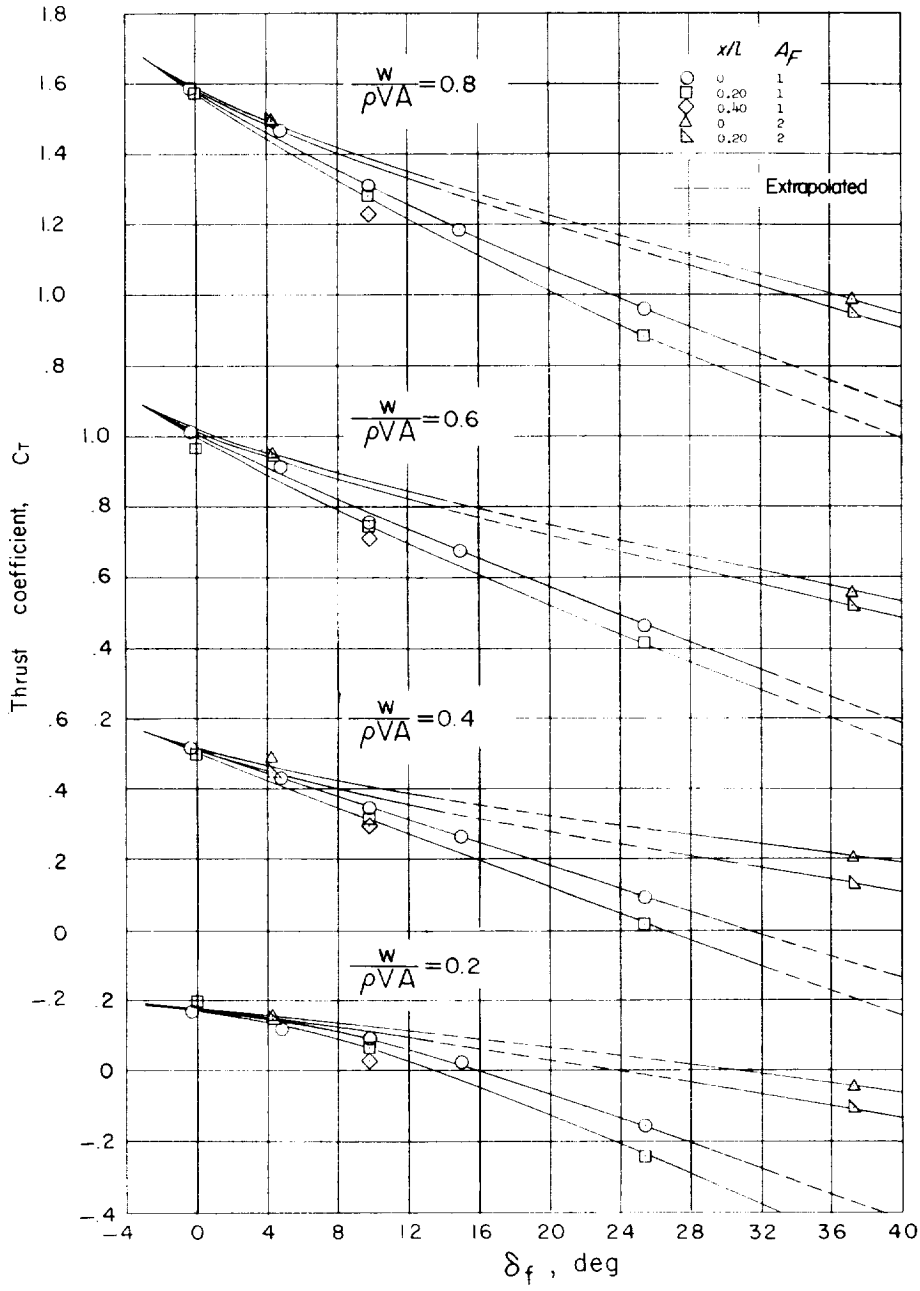

(b) Mach number = 0.70.

Figure 9.- Continued.

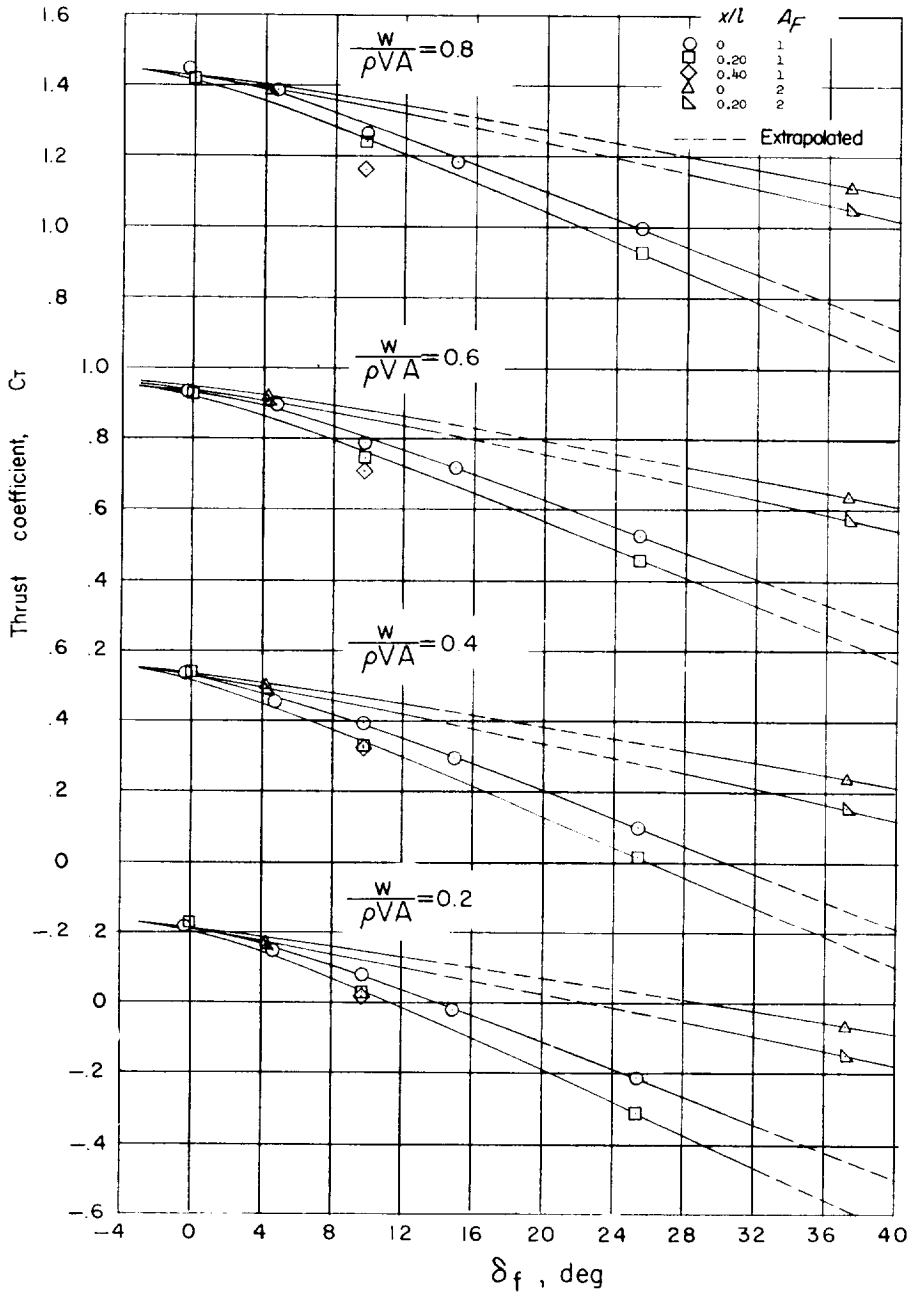

(c) Mach number = 1.00.

Figure 9.- Continued.

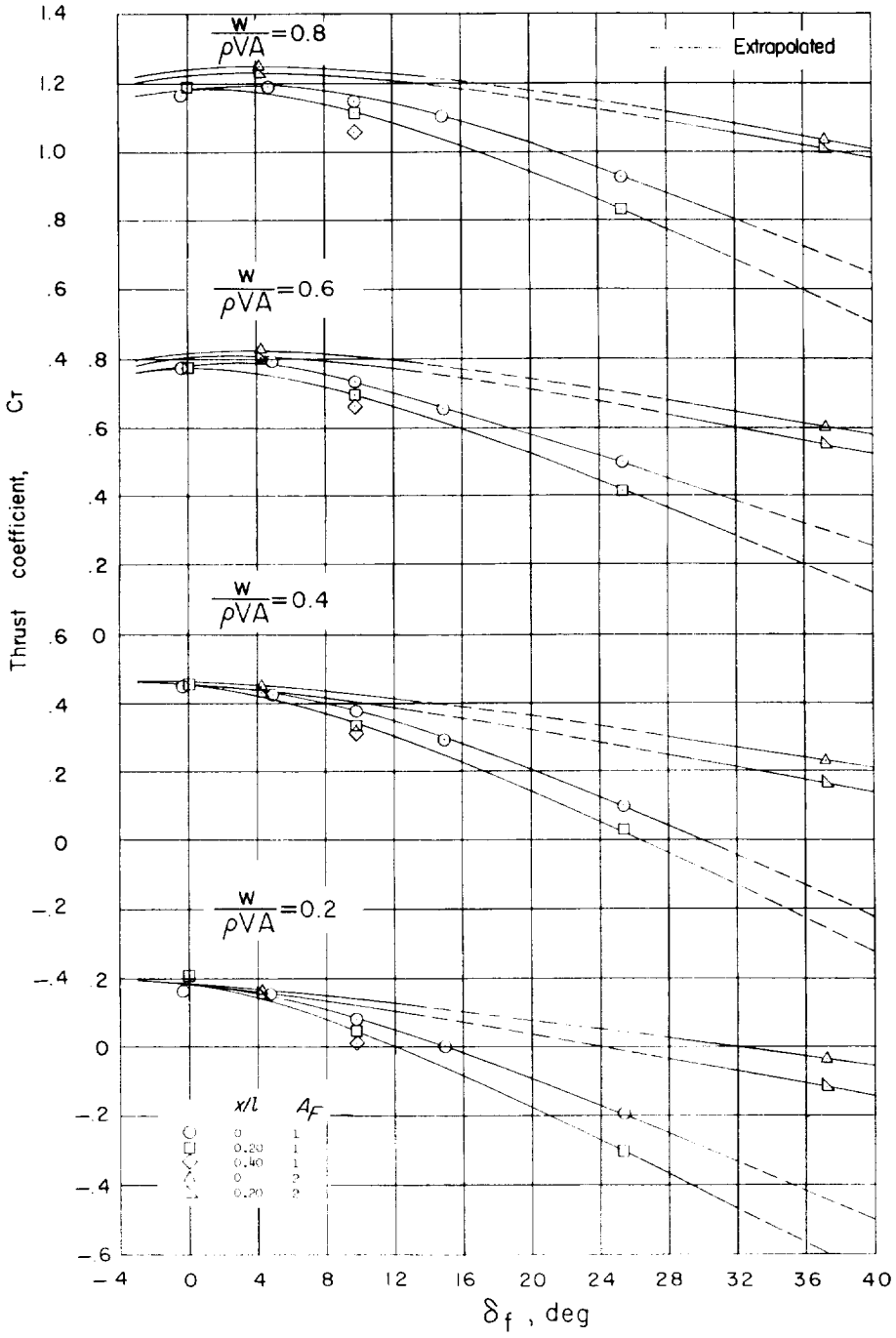

(d) Mach number = 1.30.

Figure 9.- Concluded.

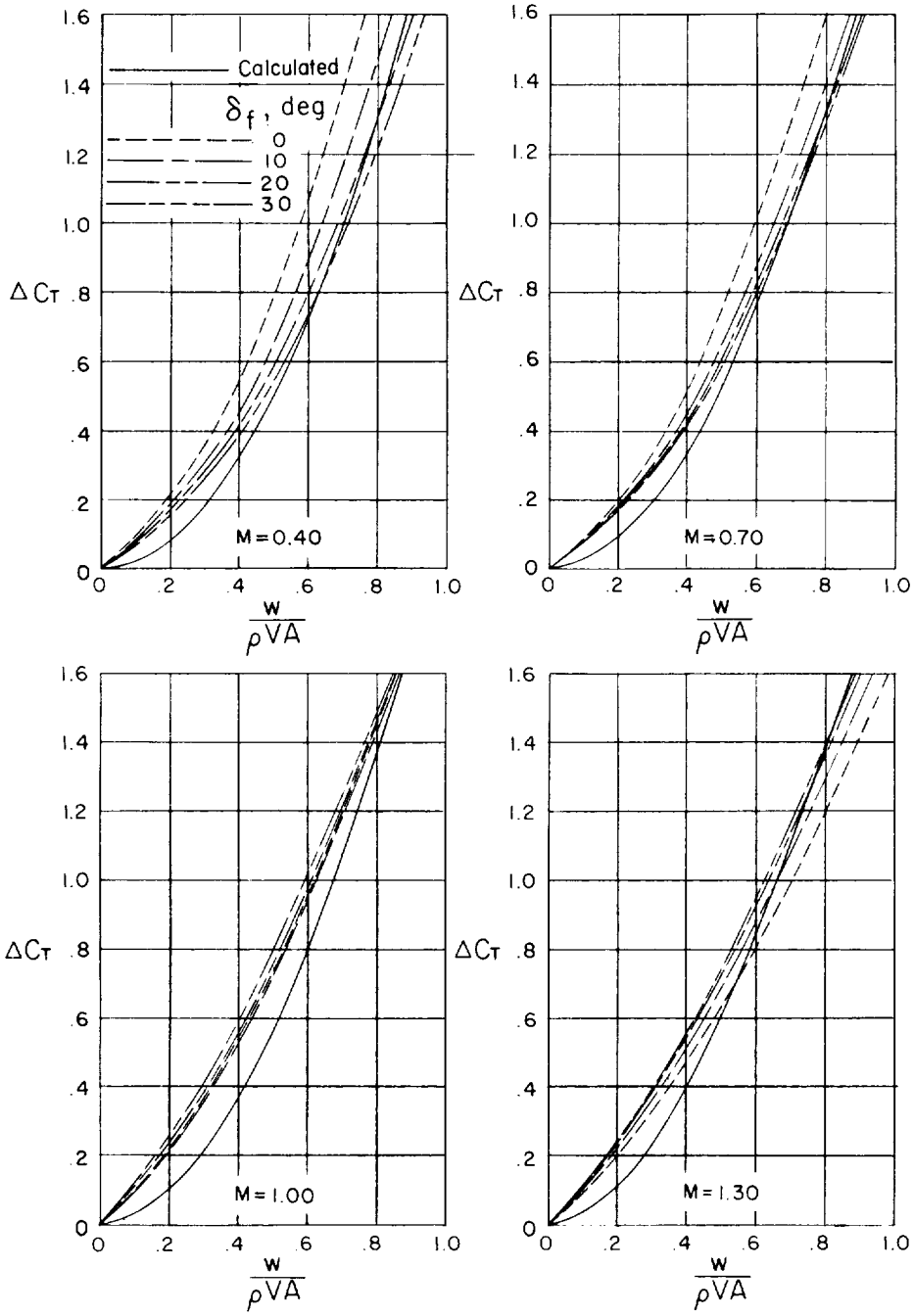

Figure 10.- Comparisons of apparent thrust produced by flapped outlets with calculated values. $A_F = 1$; $x/l = 0$.